ESR1 MUTATIONS AND ENDOCRINE RESISTANCE IN HUMAN BREAST CANCER

by
David Chu

A dissertation submitted to Johns Hopkins University in conformity with the requirements for the degree of Doctor of Philosophy

Baltimore, Maryland
March 2017

ABSTRACT

Two thirds of all breast cancers are characterized by the expression of estrogen receptor (ER) α, encoded by the gene *ESR1*. Mutations in the ligand binding domain (LBD) of *ESR1* have been identified as a resistance mechanism in patients who have progressed on endocrine therapies. In order to better understand the clinical significance of these mutations, two novel approaches for studying *ESR1* activating mutations were developed. First, we characterize the two most prevalent *ESR1* mutations, Y537S and D538G, through gene editing of the endogenous loci in ER-expressing human breast epithelial cells. In *in vitro* and *in vivo* assays, both *ESR1* Y537S and D538G knockins demonstrate estrogen independent proliferation and tumor xenograft formation. Additionally, *ESR1* mutations confer resistance to tamoxifen, fulvestrant and palbociclib but not some combination therapies. Both *ESR1* Y537S and D538G knockins are selected for under endocrine treatment when cultured with MCF7 parentals cells *in vitro*, with the *ESR1* Y537S knockin showing increased resistance compared to the *ESR1* D583G knockin. Moreover, when co-cultured together under estrogen deprived conditions, the *ESR1* Y537S knockin cells outcompete the *ESR1* D538G knockin cells, *in vitro* and *in vivo.* Taken together, these results suggest that functional modeling of *ESR1* mutations can provide insight on mechanisms for resistance, how these resistance mutations can be selected and effective drug combinations for the treatment of endocrine resistance breast cancers. Second, given the problem of tumor heterogeneity in breast cancer, the true frequency of *ESR1* mutations may be underestimated since mutational profiles can vary between different sites of metastatic disease. Here, we detect a higher frequency of *ESR1* mutations in

circulating plasma tumor DNA (ptDNA) using droplet digital PCR (ddPCR). We obtained blood from eleven patients with known *ESR1* mutational status identified by next generation sequencing of biopsied metastatic tissues. All corresponding *ESR1* mutations were detected in ptDNA, with two patients harboring additional *ESR1* mutations not present in metastatic tissues. In a prospective cohort, metastatic tissue and plasma were collected contemporaneously from eight ER-positive and four ER-negative patients. Although no *ESR1* mutations were identified in tissue biopsies, ddPCR detected seven *ESR1* mutations in ptDNA from six of the eight ER-positive patients (75%). We show that *ESR1* mutations occur at high frequency and that blood can be used to identify additional mutations not found by sequencing of a single metastatic lesion.

Thesis Advisor: Ben Ho Park, MD., Ph.D.

Thesis Readers: Ben Ho Park, MD., Ph.D.
Paula Hurley, Ph.D.

ACKNOWLEGDEMENTS

During my journey to complete my Ph.D., I have been fortunate to have the love, support, advice and guidance from my family, friends, colleagues and mentors. I feel that the level of success I've achieved in graduate school is proportional to the mentorship I have received up to this point. While there are many people I owe my deepest gratitude, I would like to take a moment to acknowledge a handful of individuals who have been instrumental in this journey.

First, I would like to thank my mentor and thesis advisor, Dr. Ben Ho Park. I am honored and humbled to have been one of your trainees. There is not one day that goes by where I forget how incredibly fortunate I am to have a mentor like you. I still remember the first time I met you during my recruitment weekend. I'm not sure whether it was your cheesy laugh, your charisma, or your scientific aura but I walked away from our conversation thoroughly impressed. I was motivated by your vision and passion for pursuing meaningful work. "This is someone I want to train under." I said to myself. Now, six years later, I can honestly say that leaving the comforts of LA and moving to Baltimore to train under you has been one of the best decisions of my life. Your generosity is unparalleled. Your enthusiasm for life is contagious. Simply put, you're a beautiful human being and I aspire to be like you one day.

It is said that friends are the family you get to choose. To the Park, Lauring and Hurley lab members, past and present, you have made this journey absolutely remarkable and incredibly enjoyable. I never imagined that I would find such a diverse cast of scientists that I can say are not only my colleagues but also my family. The last several years has been filled with laughter, joy, and the pursuit of knowledge. For that I

am truly thankful. To my friends that I've met during my time on the East coast, your friendship and support will never be forgotten. You've been instrumental in making Baltimore my new home.

To my family, thank you for understanding that my time is short whenever I come home to visit. You always welcome me with open arms and I'm forever grateful. To my two older brothers Pete and Tin, thank you for taking care of Mom in my absence. Knowing that you two are there has made my decision to pursue a doctorate across the country possible. I want to say thank you to my Mom, the woman who remains a pillar in my life. To this day, I'm still profoundly amazed by how you continue to sacrifice for your children. I may never understand the courage it took for you to leave a war-torn country for the slim possibility at a better life here in the States. Truly, this doctorate is the summation of the last 30 years you have sacrificed to build a new life for your family. I love you and hope you feel this is as much an accomplishment for you as it is for me.

Last, but certainly not least, I want to thank my girlfriend Donna. You are a reminder that, sometimes, nice guys finish first. It may have taken me 30 years to find you but now that you're here, I'm never letting go. I always believe that relationships were meant to be simple and that has never been truer than when I am with you. You may argue that you're conditioning me to become dependent on you but all of the small gestures – making me coffee in the morning, restocking my candy drawer, and picking up Subway for lunch – never go unappreciated. I'm incredibly thankful for how supportive you been during this journey. You've filled my life with happiness and I look forward to what the future holds for us. I love you.

TABLE OF CONTENTS

LIST OF TABLES

Chapter 2

Chapter 3

LIST OF FIGURES

Chapter 2

1 Introduction

Breast cancer and genetics overview

Despite cancer associated deaths steadily declining over the last two decades, breast cancer remains the most commonly diagnosed cancer in women in the United States[1]. Each year, approximately 1 in 8 women will be diagnosed with breast cancer and in 2015, there were approximately 232,000 new cases of breast cancer and 40,000 deaths. In the United States, breast cancer remains the second leading cause of death in women[2]. It is now widely accepted that breast cancer is primarily a genetic disease, influenced by both the presence of susceptibility factors and the accumulation of oncogenic changes and alterations in tumor suppressor genes[3]. Under the right conditions, these genetic alterations, including single base substitutions, amplifications, rearrangements and deletions,

enhance the fitness of a normal cell, leading to the development and growth of a tumor.

Although breast cancer is commonly summarized as a singular disease, it can be further stratified into 21 different histological subtypes depending the genes that are expressed[4]. While these classifications can provide prognostic value and who is likely to benefit from adjuvant endocrine or chemotherapy, breast cancer is commonly classified into molecular subtypes based on the presence or absence of several receptors. These receptors include estrogen receptor (ER), progesterone receptor (PR) and amplification of human epithelial growth factor receptor 2 (HER2), making up the four different subtypes: luminal A, luminal B, HER2+ and triple negative[5]. Classification of breast cancer into these subtypes has led to the understanding of how these receptors drive and promote the survival of cancer cells. More importantly, knowledge of these pathways has led to the development of specific inhibitors that can repress cancer growth.

Estrogen receptor positive breast cancer accounts for approximately 70% of all breast cancer cases. By definition, this cancer subtype is primarily driven by the hormone estrogen. Since the identification of ER in the late 1950s, endocrine therapies have been developed that modulate ER signaling through repression of downstream effectors or inhibiting the synthesis of endogenous estrogen. While these therapies have been effectively in treating women with ER-positive breast cancer, prolonged exposure to these drugs invariably leads to resistance. Recent genome sequencing studies have revealed that activating mutations in the gene

that codes for ER, *ESR1*, is responsible for acquired resistance to endocrine therapies[6-10]. *ESR1* mutations cluster in the ligand binding domain of ER and understanding how they confer drug resistance can elucidate pathways and targets that can resensitize these cells to endocrine therapies.

ESR1 background and function

Discovery of ESR1

While the nuclear hormone receptor ERα protein was not purified and isolated until the late 1970s, the role of estrogen and its receptor in breast cancer progression was well cited before its discovery. In 1896, George Beatson reported that removal of the ovaries in premenopausal women with advanced breast cancer reduced the size of tumors and improved patient's prognosis[11]. This was based on the observation that the size of a breast tumor increased and decreased during a woman's menstrual cycle, suggesting that a key regulator was derived from the ovaries. This practice would be furthered by Stanley Boyd in 1900, citing that a third of his patients with breast cancer benefited from ovarian ablation[12]. Allen and Doisy, in 1923, noticed that mice that undergone a double ovariectomy failed to exhibit periodic growth in the epithelium lining their genital tract. However, injection of ovarian extracts into mice restored growth in the genital tract, demonstrating that the steroid hormone estrogen was produced in the ovaries[13]. Estrogen receptor was first described by Elwood Jensen in 1958. Jensen utilized tritiated estradiol and found the highest amounts localized to the uterus, vagina and ovaries when injected into female mice[14]. Subsequently, in

1980, Geoffrey Greene along with Jensen, purified ER protein from human breast epithelial MCF7 cells by passing cytosolic extract through an estrogen affinity column and subsequently developed a monoclonal antibody to ER[15]. This seminal study provided the groundwork for the eventual cloning of the estrogen receptor in the mid 1980s[16-17].

ESR1 gene and protein structure

The *ESR1* gene is located on chromosome 6q25.1 and contains 10 coding exons. The *ESR1* gene has 13 different splicing variants with the dominant *ESR1* mRNA transcript variant encoding a 67 kDa nuclear receptor protein and is comprised of 595 amino acids. ERα (also known as NR3A1) belongs to a family of nuclear receptor family of transcription factors that also includes ERβ (also known as NR3A2), encoded by *ESR2*. The *ESR2* gene is located on chromosome 14q23.2 and contains 14 coding exons. *ESR2* has 13 different splicing variants but unlike *ESR1*, several splice variants are expressed in tissues. However, what is currently regarded as the wild type ERβ is 63kDa and comprised of 530 amino acids. It is important to note that although the action of estrogen is now known to be mediated through the interactions of both of these estrogen receptors, ERβ was not cloned until the mid 1990s[18]. The interaction between these two receptors and their contribution to estrogen mediated signaling is still being unraveled. Therefore, any subsequent mention of the estrogen receptor refers to ERα, unless otherwise stated.

In order to determine the different functional domains of the estrogen receptor, initial molecular cloning experiments focused on confirming the sequence of human ER cDNA and comparing it to other steroid hormone receptors for homology[16-17, 19]. These comparison studies revealed six regions of variable conservation, namely regions A to F, that helped elucidate their function. Regions A, C and E were found to be highly conserved and separated by regions of lower homology, B, D and F[20]. Region A/B and E make up the activation domains AF-1 and AF-2 domains respectively[21]. AF-2 is also known as the ligand binding domain (LBD). Upon ligand binding, ER undergoes a conformational change that facilitates that recruit a range of coregulatory proteins. Interestingly, although transcriptional activation involves the synergy between the two AF domains, only AF-2 is entirely dependent on ligand binding activity[22]. Region C is highly hydrophilic, consisting of basic amino acids and cysteines, and forms the DNA-binding domain (DBD), responsible for recognition of estrogen response elements (ERE) and DNA binding. Region D is the hinge region, linking the DBD and LBD together. Lastly, region F is important for modulating gene transcription and regulating receptor dimerization[23-24].

Estrogen signaling

Estrogen receptors are primarily activated by its cognate hormone estrogen. The most potent estrogen produced in the body is 17β-estradiol (E2). Two other metabolites of estrogen, estrone and estriol, also exist but are weaker agonists of ER. Interestingly, the binding pocket in the ligand binding domain of

ER also permits the binding of other estrogen mimetics such as phenol red as well as other environmental contaminants, allowing for downstream signaling in the absence of E2[25].

Estrogens and estrogen receptors stimulate target gene expression through two primary mechanisms: “classical” and “non-classical” signaling. During “classical” signaling, ligand binding induces receptor dimerization and transcriptional activation. Activated ER complexes are able to recognize palindromic sequences known as estrogen response elements located in the promoters of target genes. Additionally, ligand binding induces a conformational change that permits the recruitment and binding of a variety of coregulators, such as SRC1, AIB1, BCAS3 and PELP-1 that alter chromatin structure and facilitate the recruitment of RNA polymerase II for transcription initiation. Notably, the collection of co-activators and co-repressors that modulate ER signaling differ depending on the tissue type, a balance that is especially important in anti-estrogen therapy.

About a third of the genes in humans that are regulated by ER do not contain or only contain half of the ERE sequence and thus, are regulated in a “non-classical” manner[26]. During “non-classical” signaling, ER can regulate target gene expression without directly binding to DNA by tethering to other transcription factors in the nucleus. Transcription factors such as AP-1, SP-1, SF-1 and NF-κB can interact with ER, enhancing the recognition and initiation of transcription at alternative response elements[27]. This mechanism is common among other nuclear hormone receptors and is referred to as transcriptional

cross-talk[28]. Additionally, studies are increasingly demonstrating that the estrogen receptor can undergo a number of posttranslational modifications that include phosphorylation, methylation, acetylation, sumoylation and ubiquitination with the most documented being phosphorylation. Serines and tyrosines along the AF-1 and hinge domain of ERα can be activated by MAP kinase, AKT, protein kinase A, and HER2, leading to downstream signaling in the absence of ligand[29-30].

Lastly, while estrogens predominantly exert their effects through the two canonical pathways listed above, some effects of estrogen are so instantaneous that they could not be dependent on RNA activation and protein synthesis. This last category is known as non-genomic signaling and is thought to be mediated by membrane associated ER and the activation of various protein-kinase cascades[31]. The most well-studied of these non-genomic actions is through activation of the MAP kinase and phosphoinositol (PI) 3-kinase signaling cascade [32-33]. Collectively, the interactions of all of these intersecting pathways highlight the profound effects of estrogen on growth and differentiation on the different target tissues in the body.

1c. Clinical Importance of ER in breast cancer

In addition to its role in development and morphogenesis, ER has been long acknowledged as a major driver in breast cancer. Approximately 70% of all breast cancers express estrogen receptor. Studies have shown that luminal breast epithelial cells are characterized by high expression of *ESR1* whereas

other tumor types show little to no expression of this gene[34]. Thus, ER-expressing breast cancers are normally classified under the luminal subtype. Luminal breast cancers are further divided into luminal A and B, with luminal B characterized by high levels of HER2 or Ki67 cells[35]. Luminal A breast cancers have been shown to be associated with better clinical outcomes when compared to other subtypes. This is largely due to ER expression correlating with lower tumor grade, lower tumor proliferation, less amplification of HER2 oncogene, retention of the p53 tumor suppressor gene and slower rates of disease recurrence. Additionally, compared to the triple negative subtype, there are a growing number of therapies that inhibit ER and ER signaling.

Since the identification of ER in the late 1950s, it has been a subject of immense research and a target for the development of cancer therapies. Endocrine therapies for the treatment of ER-positive breast cancer work by a number of mechanisms but all aim to antagonize estrogen mediated signaling. Three types of endocrine therapies exist for the treatment of ER-positive breast cancers: selective estrogen receptor modulators (SERMs), selective estrogen receptor degraders (SERDs) and aromatase inhibitors (AI). SERMs, such as tamoxifen, bind to ER and recruit co-repressors which prevent transcriptional activation and the production of downstream effectors[36-37]. SERDs, like fulvestrant, modulates ER signaling by promoting the proteasomal degradation of ER[38]. Lastly, aromatase inhibitors regulate the amount of estrogen present by blocking the conversion of androgens to estrogens and in postmenopausal women, can result in a 98% decrease in circulating levels of estrogen[39]. In

premenopausal women, tamoxifen or ovarian suppression, either by pharmacological inhibition or surgical removal, is standard of treatment.

Identification of *ESR1* activating mutations in hormone-resistant metastatic breast cancer

While endocrine therapies remain the mainstay for the treatment of ER-positive breast cancers, approximately 30% of ER-positive breast cancers exhibit *de novo* resistance and another 40% acquire resistance to these therapies after prolonged exposure. Several clinical observations revealed that in approximately 20% of patients treated with endocrine therapies, reduced expression of ER was observed[40-41]. These findings suggest that these tumors are no longer driven by estrogen and likely that alternative pathways have been activated. Secondly, upregulation of *HER2* has been shown to be associated with insensitivity to estrogen therapies[42-43]. This is possible since data suggest that HER2 may reduce levels of ER, thus rendering a tumor less responsive to estrogen[44]. Additionally, PR is commonly loss in ER-positive breast cancer patients who are treated with endocrine therapies and PR loss has been shown to be associated with increased growth factor signaling which can subsequently downregulate ER[44-45].

Large scale sequencing projects have profoundly transformed our ability to understand cancer biology on the genetic level. In the seminal study, Wood *et al.* utilized Sanger sequencing to unravel the range and frequency of genetic alterations that make up breast and colorectal tumors, now known as the “cancer

genome landscape" [46]. Rather than stochastically distributed, the genes that are commonly mutated can be divided into two groups based on the frequency found across tumors: "mountains" which are frequently mutated and likely to drive cancer initiation and progression and "hills" which are less frequently mutated and likely harmless. These "mountains" include *TP53, PIK3CA, APC, KRAS* among many others[46-47]. It comes as a surprise that despite estrogen signaling being a key driver of ER-positive breast cancers, mutations have been largely absent in the estrogen receptor[48]. Recently, several groups shed light on a decade old conundrum in breast cancer genetics. These studies collectively highlighted that estrogen receptor did, in fact, exhibit hotspot mutations but only in patients who had metastatic ER-positive breast cancer and had progressed on endocrine therapy[6-10]. Patients who were ER-negative, were not treated with any endocrine therapies or were presented with primary disease did not exhibit these activating mutations[9]. Thus, *ESR1* mutations do not drive ER-positive breast cancer but mediate endocrine resistance. Interestingly, the idea of an *ESR1* activating mutation conferring estrogen independent transactivation was first proposed in 1997 by Suzanna Fuqua[49]. However, the small sample size of the study (n=1) and the failure of subsequent genome wide sequencing studies to identify similar lesions could possibly explain why these activating mutations have eluded discovery for such a long time[48].

Collectively, previous studies investigating the functional consequence of mutations in the ligand binding domain of *ESR1* have strongly suggested that the overexpression of these mutations induce estrogen independence and confer

resistance to endocrine therapies. Indeed, the first clue originates from a study by Li *et al.* utilizing patient derived xenograft (PDX) mouse models with tumor cells derived from primary and advance breast cancers that were resistant to endocrine therapies[6]. RNA-sequencing data from two of the PDX mice revealed the *ESR1* Y537S and E380Q mutations were present in the majority of reads. When MCF7 and T47D cells were stably transduced with lentiviral vectors to overexpress the *ESR1* Y537S mutation, both cell lines exhibited estradiol independent proliferation, although MCF7 cells retain some estradiol responsiveness. Moreover, the addition of fulvestrant only partly inhibited the proliferation of the *ESR1* Y537S mutant compared to significant inhibition in the parental cell lines.

Shortly after the study by Li *et al.*, two concurrent genome wide sequencing studies characterizing tumors from patients with advance ER-positive breast cancer treated with anti-estrogen therapies and aromatase Inhibitors revealed additional *ESR1* mutations that cluster in the ligand binding domain of ER[7-8]. In addition to the aforementioned *ESR1* Y537S mutation, the *ESR1* L536Q/R, Y537N/C, and D538G mutations were reported. Using HEK293T cells co-transfected with an ERE-firefly luciferase reporter plasmid and various *ESR1* constructs, Robinson *et al.* demonstrated strong constitutive transactivation of the ERE reporter by the *ESR1* mutants in the absence of estrogen. Moreover, it was found that although the *ESR1* mutants could be inhibited by tamoxifen and fulvestrant in a dose-dependent fashion, the IC50 was two to four fold higher for the mutants compared to cells expressing wild-type *ESR1*. Similar results were

seen by Toy *et al*. in MCF7 and SK-BR-3 cells when mutant *ESR1* was cotransfected with a luciferase report construct[8]. When nude mice were injected with MCF7 cells contained doxycycline induced vectors with these *ESR1* LBD mutations, tumors were able to establish and grow in the absence of E2 supplementation. Molecular modeling studies have demonstrated that the *ESR1* Y537S and D538G mutations induce a confirmation change in ER to favor the agonist confirmation in the absence of any ligand, suggesting constitutive activation of ER signaling[8, 10].

Isogenic modeling of *ESR1* activating mutations

To date, an emerging body of evidence has addressed the stark difference between oncogenic mutations that have been overexpressed, usually by transient or stable transfection of cDNA, or knocked in as a single copy in cell lines. In a seminal finding, Konishi *et al*. described the dramatic differences in transformation between K-*ras* G12V knock-in cells and K-*ras* G12V overexpressing cells[50]. Surprisingly, when mutant K-*ras* is knocked into MCF10A cells, a non-tumorigenic breast epithelial cell line, the phenotype was minimal yet when the same mutant K-*ras* was overexpressed, MCF10A cells were dramatically transformed, exhibited growth factor independence and downstream MAP kinase signaling. In addition, other studies have highlighted discrepancies in drug sensitivities between cell lines overexpressing mutant cDNA and single nucleotide knockin of mutant oncogenes. Notably, overexpression of the *HER2* L755S mutation in MCF10A cells conferred resistance to the tyrosine kinase

inhibitor lapatinib[51]. However, when the same *HER2* L755S mutation was endogenous expressed as a single copy in MCF10A cells, the MCF10A *HER2* L755S cells did not demonstrate any resistance phenotypes compared to parental cells[52]. Additionally, discrepancies between overexpression of mutant cDNA and single nucleotide knockin of mutant oncogenes have been seen in studies involving *EGFR* and *AKT1*[53-54].

In light of the caveats mentioned above, we sought to develop an isogenic model to study the functional consequence of a single *ESR1* activating mutation when driven by an endogenous promoter. This is critical since, to date, *ESR1* mutations have not been found to be associated with amplification of the *ESR1* gene and a more clinically relevant model is needed[8]. Additionally, it has been appreciated that oncogenic changes can cooperate and lead to a more transformed phenotype[55-56]. However, how single knockins can interact with each other has not been well characterized. Here, we utilize the ER-expressing breast epithelial cell line, MCF7, to create single, heterozygous *ESR1* mutants. In this study, we focus on the two most common *ESR1* mutations, *ESR1* Y537S and D538G, to investigate their effects on proliferation, tumor formation, estrogen independence and resistance to endocrine therapies. Additionally, we evaluated the sensitive of these knockins to the CDK 4/6 inhibitor, palbociclib, singly and in combination with SERDs and SERMs, since palbociclib has recently been shown to be preferentially inhibit the proliferation of luminal ER-expressing breast cancer cell lines *in vitro*[57]. We also model how these mutations can arise under estrogen deprivation and drug selection. Lastly, we demonstrate that although

mutations are found on adjacent codons in the LBD, their transformative properties are not identical.

2 Isogenic modeling of *ESR1* activating mutations

Introduction

Estrogen receptor α (ERα) belongs to a nuclear receptor family of transcription factors and is expressed in ~70% of all breast cancer cases. Classically, activation of ER signaling leads to the transcription of target genes that regulate a wide array of cellular functions that include proliferation, differentiation, migration and cell survival. Identification of the estrogen receptor has led to the development of endocrine therapies, such as tamoxifen and fulvestrant, which directly inhibit ER signaling. In addition to anti-estrogen therapies, aromatase inhibitors that suppress the production of estrogen, such as exemestane and letrozole, are standard of care in post-menopausal women. Inhibitors that suppress estrogen-driven signaling have been shown to be highly effective[58].

Despite many ER-positive breast cancer patients responding to these drugs, prolonged exposure invariably lead to resistance. Approximately 30% of ER-positive breast cancers exhibit *de novo* resistance with an additional 40% acquiring resistance to these therapies[59]. Genome wide sequencing studies involving metastatic breast cancer patients who have progressed on endocrine therapies have revealed activating mutations in the ligand binding domain (LBD) of the *ESR1* gene[6-10]. Collectively, these studies demonstrate that overexpression of these activating mutations induces estrogen independent transcription and partial resistance to tamoxifen and fulvestrant.

Past studies have highlighted discordant results between single nucleotide knockin of mutant oncogenes and overexpression of mutant cDNA[50, 53, 60]. Notably, the *HER2* L755S mutation confers resistance to the tyrosine kinase inhibitor lapatinib when overexpressed but not when endogenously expressed[51-52]. In light of these results, we sought to investigate the effects of the two most prevalent *ESR1* activating mutations, Y537S and D538G, on transformation when driven by an endogenous promoter. Here we utilize adeno-associated viral mediated gene targeting to knock in these *ESR1* mutations into a human ER-positive breast epithelial cell line to examine the effects on transformation, drug resistance, and how these mutants can arise under selective pressures.

Results

Gene targeting of single copy, heterogeneous ESR1 activating mutations in a ER-positive human breast epithelial cell line

In order to model the effects of *ESR1* mutations found in ER-positive breast cancers, gene targeting was performed using recombinant adeno-associated virus (AAV) in the MCF7 human breast epithelial cell line. MCF7 is a cell line that was derived from a metastatic pleural effusion in a patient with ER-positive breast cancer and does not contain any activating mutations in *ESR1*[61]. One AAV gene-targeting vector was used as a backbone to introduce the two most prominent mutations, *ESR1* Y537S and D538G, in the ligand binding domain of *ESR1* (Figure 2.1A and 2.1B). In each gene targeting experiment, two independently derived clones were isolated for each *ESR1* mutations. Additionally, to control for any potential phenotypic differences caused by gene targeting, two independently derived targeted wild-type (TWT) clones were generated. Sanger sequencing as well as droplet digital PCR was used to verify the incorporation of a single copy of each *ESR1* mutation, a 50:50 biallelic ratio, and cDNA expression (Figure 2.2A and 2.2B). The cell lines generated and used in this study can found in Table 2.1.

ESR1 Y537S and D538G mutations confer estrogen independence in vitro and in vivo

Overexpression studies have demonstrated that *ESR1* Y537S and D538G mutations induce ligand independent transcriptional activation and estradiol independent growth[6-10]. In order to assess whether single copies of *ESR1* Y537S and D538G can induce estradiol independent proliferation, we performed growth

assays on our MCF7 *ESR1* mutants. MCF7 cells require estradiol present in media for robust proliferation in culture.

We found that both MCF7 *ESR1* Y537S and D538G cells proliferate in serum supplemented media without estradiol compared to MCF7 parental and MCF7 TWT cells (Figure 2.3A). In the presence of 1nM β-estradiol (E2), MCF7 parental cells show proliferation rates similar to MCF7 *ESR1* Y537S and D538G cells (Figure 2.3B). Interestingly, addition of 1nM estradiol did not increase the proliferation of either MCF7 *ESR1* mutant cells. Additionally, higher doses of estradiol do not stimulate any increased proliferation (data not shown).

MCF7 cells are able to form tumor xenografts in athymic nude mice in the presence of estradiol supplementation. Previously, it has been reported that stably transfected MCF7 cells expressing mutant ER were able to induce tumor growth after removal of estradiol pellets[7]. To investigate whether or not single copies of *ESR1* Y537S or D538G can induce ligand independent tumor formation, we injected the MCF7 *ESR1* mutant cells into nude mice. We found that both MCF7 *ESR1* mutant cells, but not MCF7 or MCF7 TWT cells, are able to form tumor xenografts in the absence of estradiol supplementation (Figure 2.4A). However, in the presence of estradiol supplementation, MCF7 wild type and MCF7 *ESR1* mutant cell lines are able to form dramatically larger xenografts when compared to xenografts formed in the absence of estradiol supplementation, suggesting that MCF7 wild type and MCF7 *ESR1* mutant cells are still estrogen responsive *in vivo* (Figure 2.4B). Taken together, this data

suggest that MCF7 *ESR1* Y573S and D538G mutations confer estrogen independence in ER-positive breast epithelial cells.

Activating mutations in the ligand binding domain of *ESR1* were found in metastatic patients who had prolonged exposure to aromatase inhibitors, that is, in an estrogen depleted environment. In order to recapitulate how *ESR1* mutants would be selected under estrogen deprivation, MCF7 cells were cultured together *in vitro* with either MCF7 *ESR1* Y537S or MCF7 *ESR1* D538G cell lines at a 1:1 ratio in serum supplemented media with and without estradiol. After 3 weeks, both MCF7 *ESR1* Y537S and MCF7 *ESR1* D538G cell lines were able to completely outcompete MCF7 cells when grown in serum supplemented media without E2 (Figure 2.5A). When grown in serum supplemented media with 1nM E2, MCF7 and both MCF7 *ESR1* knock in cells were present in equivalent proportions (Figure 2.5B). Moreover, we wanted to see if the *ESR1* mutants would thrive in an estrogen depleted environment *in vivo*. When the MCF7 *ESR1* mutant cell lines were co-inoculated in mice with MCF7 cells at a 1:1 ratio, both MCF7 *ESR1* mutant cell lines were found to be the dominant population in the tumor xenografts that were harvested (Figure 2.6A). Interestingly, when MCF7 *ESR1* mutant cell lines are co-inoculated with MCF7 cells in mice supplemented with estradiol, both cell lines are represented in the xenograft but MCF7 cells were found to be the dominant population (Figure 2.6B).

ESR1 Y537S and D538G mutations confer resistance to endocrine therapies and CDK4/6 inhibitors in vitro

Since mutations at the 537 and 538 residue of ER can induce ER transcriptional activation and estradiol independent growth, it was postulated that SERMs and SERDs such as tamoxifen and fulvestrant respectively, might still be effective at inhibiting mutant ERα. Previous overexpression studies noted that while *ESR1* Y537S and D538G mutations do confer resistance to antiestrogens, higher doses of antiestrogens are needed to bring ER transcriptional activity levels close to that of wild type ERα via a luciferase reporter assay[7-10]. Therefore, we wanted to investigate whether tamoxifen and fulvestrant can inhibit MCF7 *ESR1* mutant cell line proliferation.

MCF7 wild type and MCF7 *ESR1* mutant cell lines exhibit a dose dependent response to increasing doses of fulvestrant but both MCF7 *ESR1* mutant cells are notably more viable in the presence of 1nM fulvestrant compared to MCF7 wild type cells (Figure 2.7A). Similarly, MCF7 wild type and MCF7 *ESR1* mutant cells demonstrate a dose dependent response to tamoxifen with MCF7 *ESR1* mutants demonstrating increased viability when treated with 10nM tamoxifen compared to MCF7 wild type cells (Figure 2.7B). Consistent with previous reports, while the *ESR1* Y537S and D538G mutation confers partial resistance to tamoxifen and fulvestrant, higher doses are able to reduce viability to levels similar to MCF7 wild type cells.

Palbociclib, a selective inhibitor for cyclin dependent kinase (CDK) 4 and 6, has been shown to effectively inhibit luminal ER-positive cell lines but not

nonluminal/basal subtypes in the preclinical setting[57]. Recently, the PALOMA-3 clinical trial involving hormone receptor positive/HER2 negative metastatic breast cancer patients who have progressed on endocrine therapies demonstrated that the combination of palbociclib with fulvestrant improved progression free survival compared to fulvestrant plus placebo[62]. We wanted to investigate whether *ESR1* activating mutations influence sensitivity to palbociclib. Interestingly, both MCF7 *ESR1* Y537S and D538G mutant cells were more viable at 10nM and 100nM of palbociclib when compared to MCF7 wild type cells (Figure 2.8). MCF7 *ESR1* mutant cell lines only returned to MCF7 wild type levels when treated with 1uM of palbociclib. Notably, the addition of 1nM fulvestrant to palbociclib was able to completely inhibit both MCF7 *ESR1* Y537S and D538G mutant cells to MCF7 wild type levels (Figure 2.9A). However, the combination of palbociclib with tamoxifen was not effective in inhibiting the MCF7 *ESR1* mutants (Figure 2.9B). To ensure that *ESR1* mutations did not confer a broad resistance to chemotherapies, MCF7 *ESR1* Y537S and D538G were exposed to low doses of paclitaxel. At 10nM of paclitaxel, MCF7 *ESR1* Y537S and D538G mutant cells exhibited similar sensitivities compared to MCF7 wild type cells (Figure 2.10).

ESR1 Y537S mutant cells are more resistant to endocrine therapies than ESR1 D538G in co-cultures

In order to further model how *ESR1* mutations can arise from under selection by endocrine therapies, we cultured MCF7 parental cells *in vitro* with both MCF7 *ESR1* mutant cell lines at a 1:1 ratio in serum supplemented media

containing 1nM E2 with either 10nM tamoxifen or 1nM fulvestrant. Concordant with Figure 2.7A and 2.7B, both MCF7 *ESR1* Y537S and D538G cell lines were selected under anti-estrogen therapies after three to four weeks (Figure 2.11A and 2.11B). Interestingly, after 3 weeks MCF7 *ESR1* Y537S mutant cells were found to be selected at a quicker rate compared to MCF7 *ESR1* D538G mutant cells. MCF7 parental and MCF7 *ESR1* D538G mutant co-cultures were grown for an additional week but the ratios of wild type to D538G mutants remained unchanged (Figure 2.11B). Additionally, the fraction of MCF7 *ESR1* Y537S mutant cells were found at a higher percentage in co-inoculations compared to MCF7 *ESR1* D538G mutant cells (Figure 2.6B). These results suggest that the *ESR1* Y537S mutation may confer a more oncogenic phenotype compared to the *ESR1* D538G mutation.

ESR1 Y537S outcompete ESR1 D538G in vitro and in vivo

To determine whether the *ESR1* Y537S mutation is more activating compared to the *ESR1* D538G mutation, MCF7 *ESR1* Y537S and MCF7 *ESR1* D538G cell lines were cultured together in serum supplemented media with and without estradiol. When co-cultured in serum supplemented media, MCF7 *ESR1* Y537S cells are able to outcompete MCF7 *ESR1* D538G cells (Figure 2.12A). However, when these co-cultures are grown in serum supplemented media with estradiol, both cell lines are found at equal ratio, suggesting potential differences in ligand independent signaling between the *ESR1* Y537S and *ESR1* D538G mutants when cultured together.

In order to address any difference in proliferation rates not seen in cell proliferation assays (Figure 2.3A and 2.3B), MCF7 *ESR1* Y537S and MCF7 *ESR1* D538G cell lines were cultured separately in serum supplemented media with and without estradiol. When both MCF7 *ESR1* mutant cell lines were harvested independently and combined at 1:1 volumes, both cell lines were found at equal ratios, implying that the increased competition of the *ESR1* Y537S mutation compared to the *ESR1* D538G mutation is not due to differences in proliferation rates (Figure 2.12B). Further, in order to see if this difference could be seen *in vivo*, MCF7 *ESR1* Y537S mutant cells were co-inoculated with the MCF7 *ESR1* D538G cells in mice with and without estradiol supplementation. Under both conditions, MCF7 *ESR1* Y537S were found at a higher percentage compared to the MCF7 *ESR1* D538G cells (Figure 2.13A and 2.13B). Notably, cells that were inoculated subcutaneously in mouse 14 did not form a large tumor (data not shown) and the ratios between the MCF7 *ESR1* Y537S and *ESR1* D538G mutants were nearly equivalent, hinting that the competition between the *ESR1* Y537S and D538G mutant is, at least in part, mediated by the interaction between both mutant cell lines.

Increased competition of ESR1 Y537S mutant compared to ESR1 D538G mutant is not through paracrine signaling

Since MCF7 *ESR1* Y537S cells were able to outcompete the MCF7 *ESR1* D538G cells when cultured in serum supplemented media *in vitro*, we wanted to investigate whether this phenotype was mediated through paracrine signaling or

cell-cell interaction via transwell experiments. By two weeks, MCF7 *ESR1* Y537S cells outcompeted MCF7 *ESR1* D538G cells at a 3:1 ratio (Figure 2.12A). When MCF7 *ESR1* Y537S and MCF7 *ESR1* D538G were cultured in transwells with MCF7 *ESR1* Y537S on plates, both the MCF7 *ESR1* Y537S and MCF7 *ESR1* D538G cells were found to be lower but the MCF7 *ESR1* D538G cells were not found at the expected 3:1 ratio (Figure 2.14A). Additionally, to control for proliferation differences on transwells and plates, MCF7 *ESR1* D538G cells were grown on plates with both *ESR1* mutants grown in transwells. No appreciable difference was observed between MCF7 *ESR1* Y537S and MCF7 *ESR1* D538G cells cultured on transwells with MCF7 *ESR1* D538G cells grown on plates (Figure 2.14B). These results suggest that a diffusible paracrine factor is likely not mediating the increased competition of MCF7 *ESR1* Y537S cells when cultured together with MCF7 *ESR1* D538G cells.

ESR1 Y537S cells outcompete ESR1 D538G cells through growth suppression

Since MCF7 *ESR1* Y537S cells were found in a higher fraction when cultured together with MCF7 *ESR1* D538G cells, we wanted to assess whether this was a growth stimulatory effect on the MCF7 *ESR1* Y537S cells, a growth suppressive effect on the MCF7 *ESR1* D538G cells or a combination of both. In order to address this, MCF7 *ESR1* Y537S and D538G cells were plated singly or cultured together in serum supplemented media and grown for two weeks without passaging. After two weeks, the total amount of MCF7 *ESR1* Y537S and MCF7 *ESR1* D538G cells found in the co-cultures were found to be lower compared to

their respective single cultures (Figure 2.15). However, MCF7 *ESR1* D538G cells were found dramatically lower than the MCF7 *ESR1* Y537S cells, suggesting that both *ESR1* cell lines suppress the other mutant cell line but the MCF7 *ESR1* D538G cells were more suppressed.

Discussion

While targeted drugs such as tamoxifen and fulvestrant that antagonize ER have been highly effective therapies in the treatment of luminal breast cancer, acquired resistance after prolonged exposure remains a major hurdle to curative treatment. It has been understood that reduced expression of ER, the upregulation of HER2 and activation of other escape signaling pathways have been shown to be associated with insensitivity to anti-estrogen therapies[40-43]. Recently, the discovery of activating mutations in the LBD of *ESR1* has garnered interest due to their potential role in endocrine resistance. These studies have highlighted that mutations at the 537 and 538 residue of ER are able to induce ligand independent transcription and partial resistance to anti-estrogen therapies[6-10]. Indeed, understanding how these *ESR1* mutations are selected, promote transformation, and confer resistance to endocrine therapies permit opportunities for the development of novel therapies and drug combinations to overcome endocrine resistance.

Notably, *ESR1* mutations can induce endocrine resistance when mutant *ESR1* cDNA is overexpressed and driven by a non-endogenous promoter. While these overexpression approaches underscore the importance of *ESR1* mutations

as a resistance mechanism, they potentially overestimate the degree of endocrine resistance that would be found in breast tumors that are hormone refractory[63]. Importantly, studies investigating resistance to lapatinib have demonstrated that the *HER2* L755S mutation imparts resistance when overexpressed but not when it is endogenously expressed as a single copy[51-52]. Moreover, overexpression of mutant *KRAS*, but not single knock in, is able to induce cellular transformation and tumor formation[50, 55]. In light of this, we sought to develop a more clinically relevant model where *ESR1* mutations are not overexpressed. Here, we utilized AAV-mediated gene targeting to knock in the *ESR1* Y537S and D538G mutation into an ER-expressing breast cell line model to analyze the effect on transformation and endocrine resistance when driven by an endogenous promoter. Both *ESR1* Y537S and D538G mutants demonstrate ligand independent proliferation and tumor xenograft formation without estrogen supplementation. Interestingly, tumor xenografts formed by the MCF7 *ESR1* Y537S and D538G mutants in the presence of estrogen supplementation were significantly larger, suggesting that the both *ESR1* mutants are still estrogen responsive *in vivo* and can likely be inhibited by anti-estrogen therapies. Consistent with previous reports, the *ESR1* Y537S and D538G mutations confer partial resistance to tamoxifen and fulvestrant but are inhibited at higher doses[6-8, 10]. However, it is unclear whether the dose of tamoxifen and fulvestrant given to patients is high enough to inhibit the proliferation of these mutant cells. Indeed, our study demonstrates *ESR1* Y537S and D538G mutants can be selected for when treated with non-lethal doses of fulvestrant or tamoxifen and may require

more potent ER antagonists or other combinations therapies to circumvent drug resistance.

Clinical trials have highlighted the effectiveness of combining the CDK4/6 inhibitor, palbociclib, with either letrozole or fulvestrant in the treatment of ER-positive breast cancers[62, 64]. Palbociclib has been shown to be effective in targeting luminal breast cancer cell lines *in vitro*[57] and to the best of our knowledge, our study is the first to highlight that the *ESR1* Y537S and D538G mutations also confer resistance to palbociclib. While a patient derived xenograft (PDX) tumor model containing the *ESR1* D538G mutation was found to be resistant to palbociclib, immunohistochemistry analysis revealed a loss of Rb expression which has been attributed for the lack of response[65]. In our study, *ESR1* LBD mutants demonstrate resistance when treated with either fulvestrant or palbociclib alone but are sensitive to the combination of these two drugs. Notably, the addition of fulvestrant to palbociclib more potently inhibits *ESR1* mutants compared to tamoxifen and palbociclib. We hypothesize that the combination of fulvestrant with palbociclib target different molecular pathways compared to the combination of tamoxifen and palbociclib, but further work is needed to test this hypothesis. Ongoing clinical work will reveal whether this combination is effective in treating patients harboring *ESR1* mutations.

It is now well appreciated that different somatic alterations within the same gene can induce significant differences in transformation and response to targeted therapies[66-67]. Interestingly, despite both *ESR1* Y537S and D538G mutations being found in the ligand binding domain, our study illustrates that the

ESR1 Y537S mutant is more activating *in vitro* and *in vivo* when coupled with *ESR1* D538G mutant. Recent reports investigating the biophysical and structural biology of the *ESR1* Y537S and D538G mutations have identified differences in binding affinity to co-activators[68]. In the absence of ligand, the *ESR1* Y537S protein binds the steroid receptor coactivator 3 nuclear receptor domain (SRC3 NRD) with significantly increased affinity compared to the *ESR1* D538G protein. It is possible that this differential binding affinity to co-activators in the absence of estrogen is responsible for the increased competition we observed when *ESR1* Y537S cells are cultured with *ESR1* D538G mutant cells. Further work is required to clarify whether these differential binding affinities can be exploited therapeutically but suggest our isogenic cell lines can be utilized to development and testing of mutation specific targeted therapies.

There are limitations to this study, notably the usage of only one ER-positive breast cancer cell line to generate our *ESR1* mutant panel. Moreover, MCF7 cells contain two copies of the activating *PIK3CA* E545K mutation and one wild type copy of *PIK3CA* and knock in of the *PIK3CA* E545K in a cell line model has been shown to induce PI-3 kinase and MAP kinase signaling[69-70]. As such, it is important to examine the effects of these *ESR1* mutations on transformation and endocrine resistance in the context of the MCF7 genome. Mutant *PIK3CA* has been shown to cooperate with oncogenic changes in *TP53* and *HER2* and it is feasible to imagine cooperativity between mutant *PIK3CA* and *ESR1* on transformation and drug resistance[52, 71]. However, previous studies have cited patients harboring both a *PIK3CA* and *ESR1* mutation, providing evidence that

this isogenic model is still clinically relevant [6, 8]. In conclusion, our study utilizing an isogenic model cell line model to study *ESR1* mutations suggest that a single mutant copy of *ESR1* is sufficient to induce estrogen independent proliferation and tumor formation. While *ESR1* mutations confer resistance to anti-estrogen therapies and CDK4/6 inhibitors, they are sensitive to combination therapies, specifically the combination of fulvestrant and palbociclib. Additionally, our study demonstrates that although both *ESR1* mutations are found in the same domain and induces resistance to endocrine therapies, they confer differential degrees of transformation. This has important clinical considerations for the development of targeted mono- and combination therapies for the treatment and prevention of endocrine resistance breast cancers.

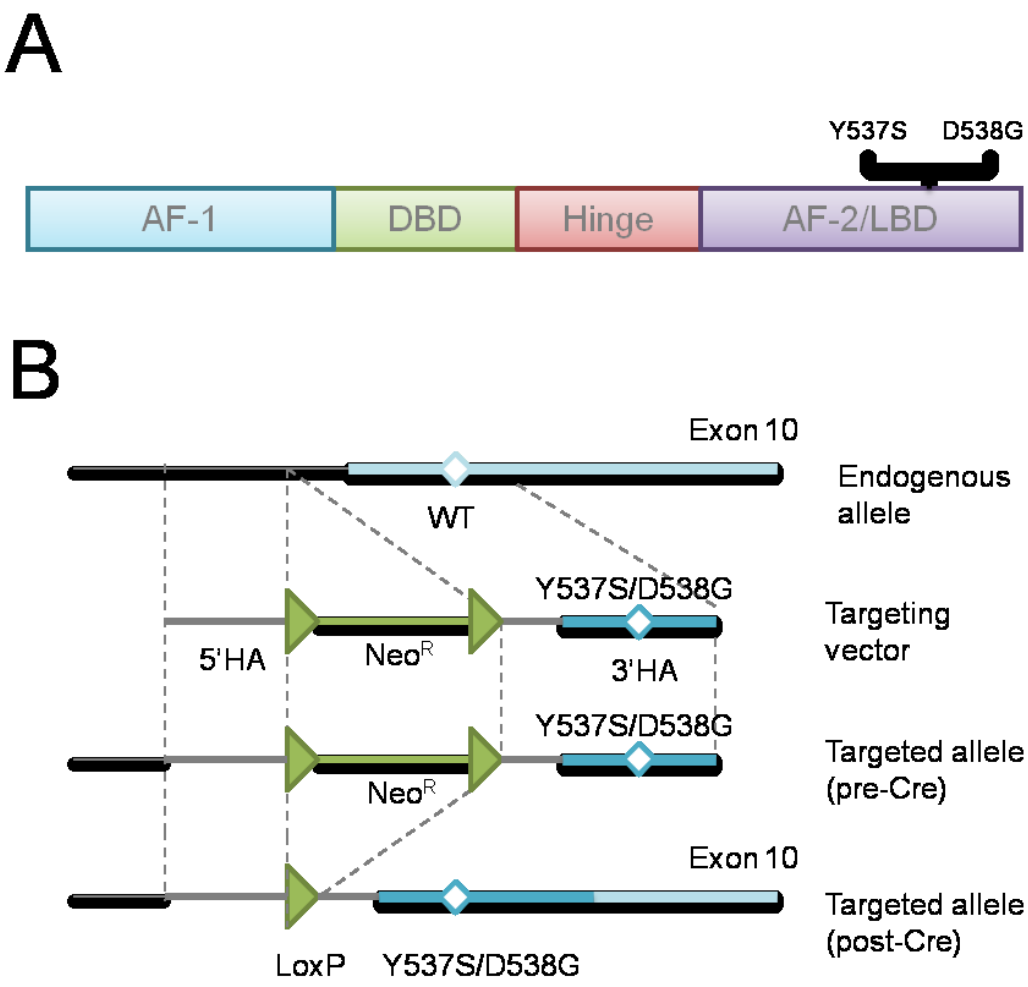

Figure 2.1: A) Diagram of ERα domains and location of knock in mutations. Abbreviations: AF-1, activation function 1; DBD, DNA binding domain; Hinge, hinge domain; AF-2 activation function 2; LBD ligand binding domain. B) Schematic of rAAV-mediated gene targeting of exon 10 of *ESR1*. rAAV transduction leads to locus specific targeting via homologous recombination of the 5' and 3' homology arms (HA). After selection with neomycin, the isolated clone is subjected to Cre recombinase for the removal of the Neomycin cassette, resulting in a LoxP site (triangle).

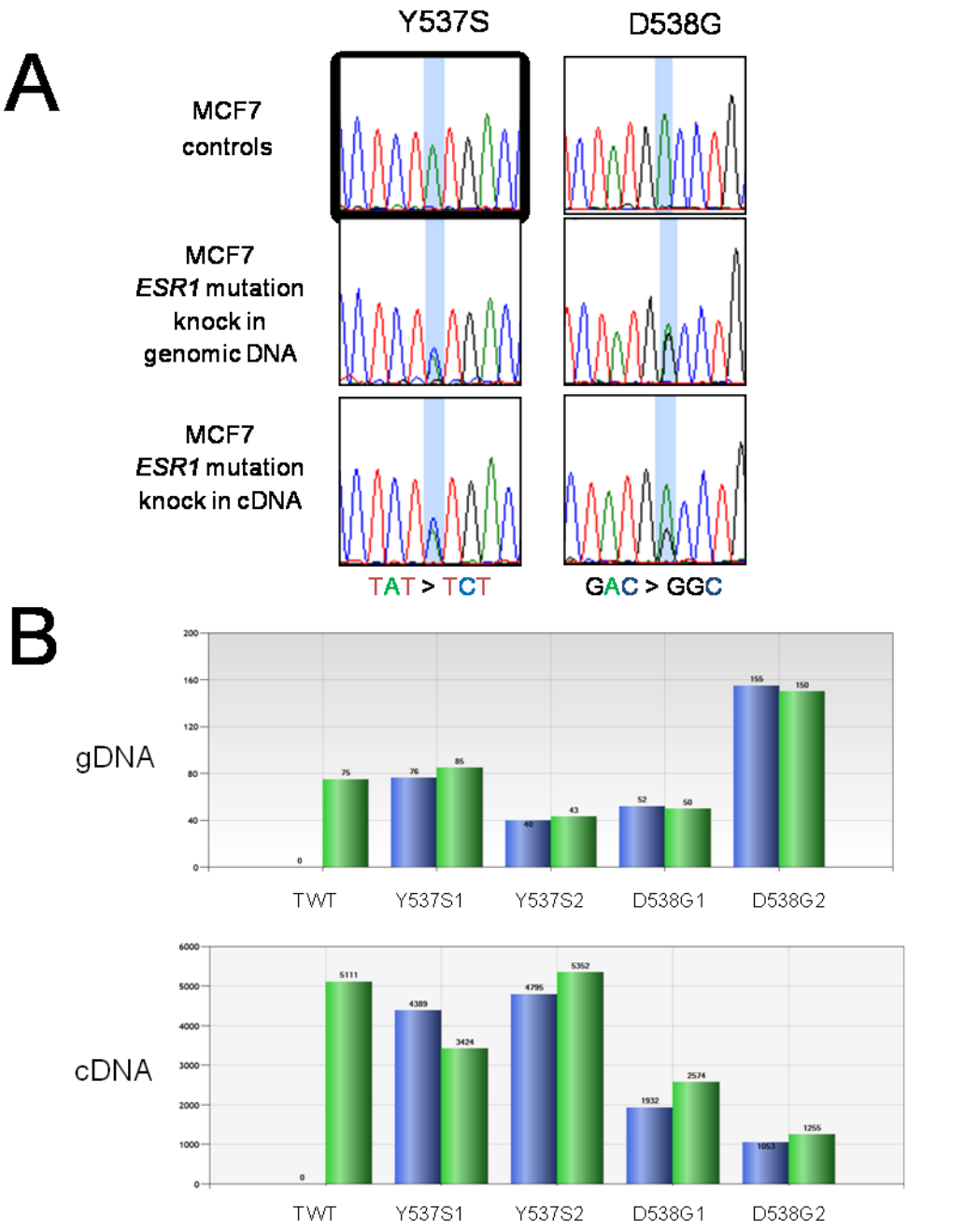

Figure 2.2: A) Sanger sequence confirming the integration of the Y537S and D538G mutation into the *ESR1* gene. Representative genomic DNA sequence traces for MCF7 parental cell lines (top), *ESR1* heterozygous mutant knock in cell lines (middle) and cDNA sequences traces for the *ESR1* heterozygous mutant knock in cell lines (bottom). B) Droplet digital PCR histograms for the *ESR1* heterozygous mutant knock in cell lines. Blue bars represent Y537S or D538G mutant probes for the targeted allele and green bars represent a wild type probe for the non-targeted allele.

A

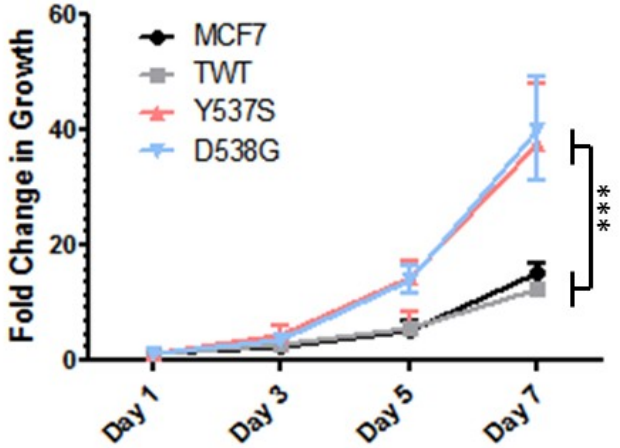

B

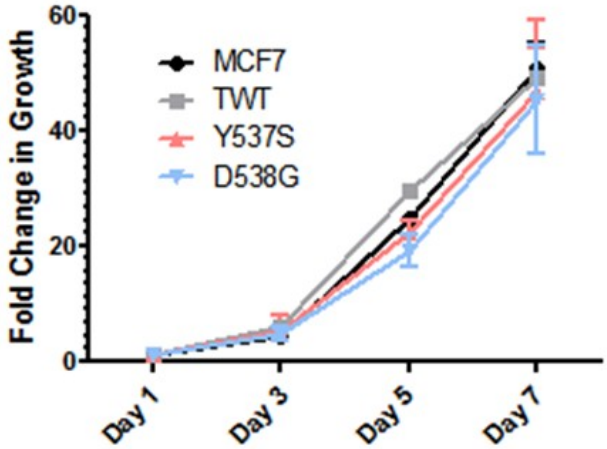

Figure 2.3: Relative proliferation for MCF7 ESR1 mutants in serum supplemented (A) and serum supplemented media supplemented with 1nM E2 (B). *ESR1* mutant cell lines are averages of two independent clones. Data are representative of the mean + SEM relative to each cell line's day 1 measurement ($n \geq 3$, $^{***}P \leq 0.001$, 2-way ANOVA followed by Bonferroni multiple comparison test).

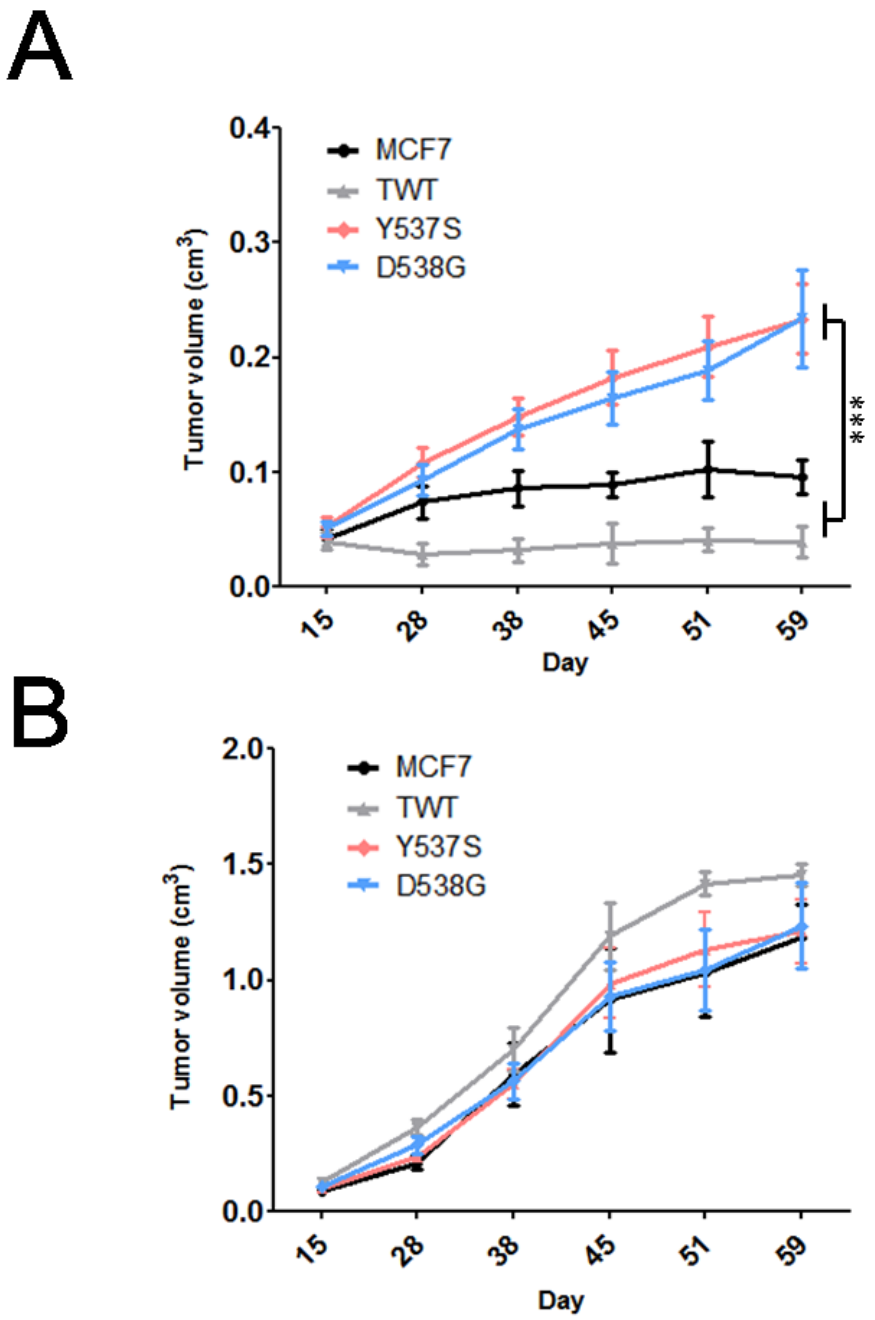

Figure 2.4: In vivo tumor growth of MCF7 *ESR1* mutants in mice supplemented without (A) and with (B) estrogen pellet supplementation. *ESR1* mutant cell lines are averages of two independent clones. Data are represented as the mean + SEM ($n \geq 5$, ***$P \leq 0.001$, 2-way ANOVA followed by Bonferroni multiple comparison test).

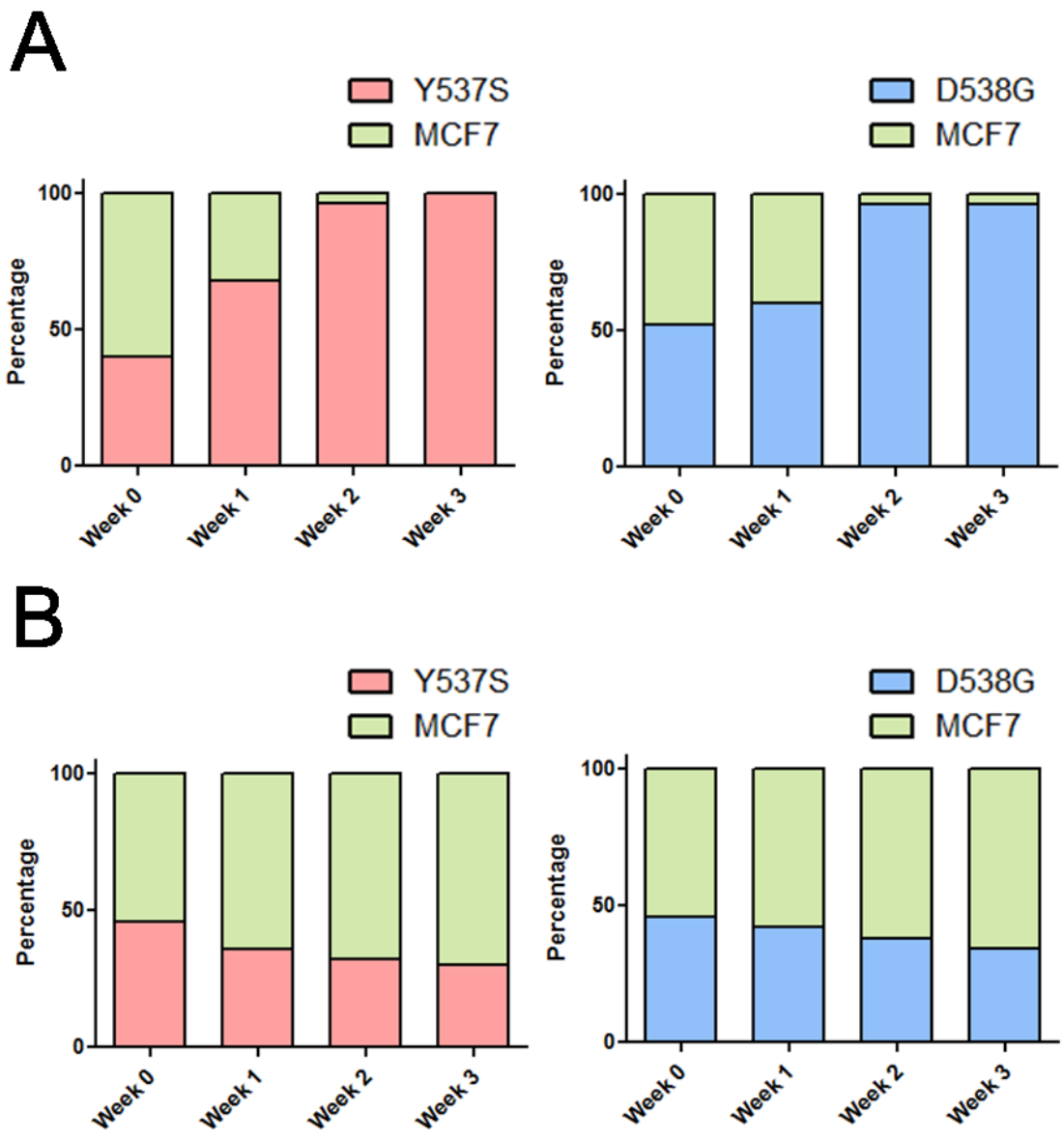

Figure 2.5: MCF7 parental and MCF7 *ESR1* Y537S and D538G mutants were co-cultured in serum supplemented (A) and serum supplemented media with 1nM E2 (B). Genomic DNA was isolated every 7 days and analyzed via ddPCR. Bars represent the ratio of MCF7 parentals to MCF7 *ESR1* mutants. Two independent experiments were performed.

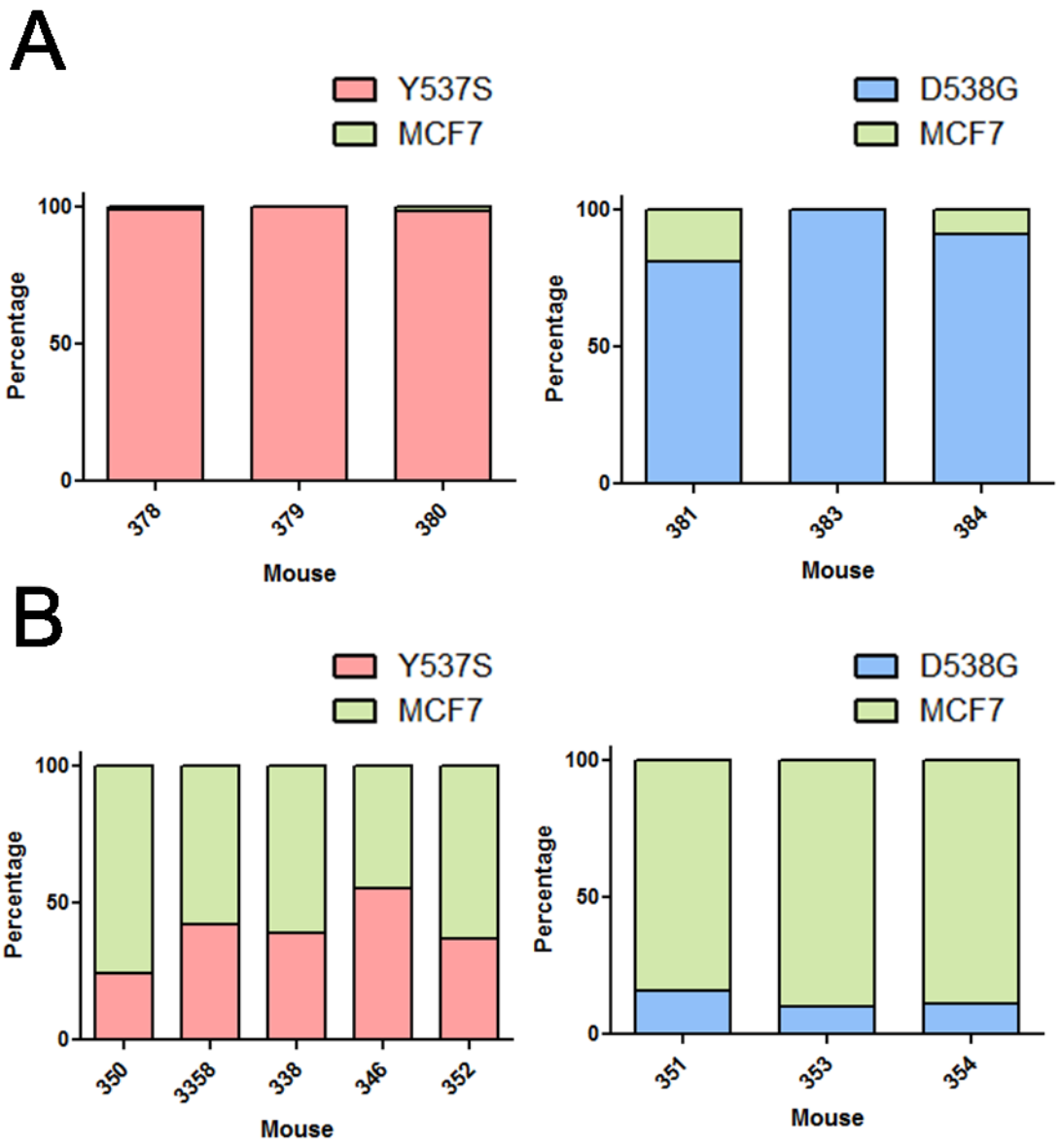

Figure 2.6: MCF7 parental and MCF7 *ESR1* Y537S and D538G mutants were co-inoculated in mice without (A) and with (B) E2 pellet supplementation. Tumors were harvested when volumes reached approximately 300mm^3. Genomic DNA was isolated and analyzed via ddPCR. Bars represent the ratio of MCF7 parentals to MCF7 *ESR1* mutants.

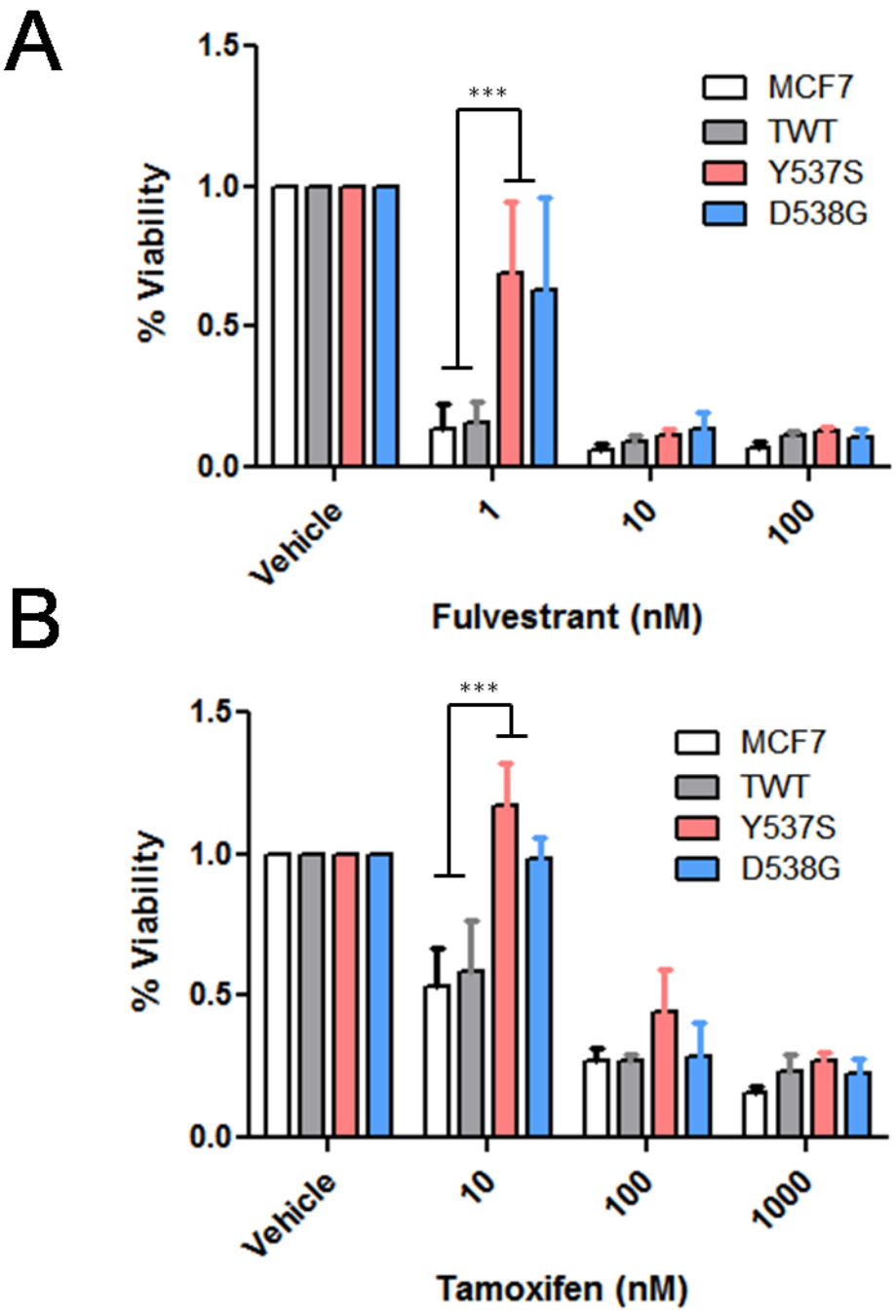

Figure 2.7: MCF7, MCF7 TWT and MCF7 *ESR1* mutants treated with fulvestrant (A) or tamoxifen (B) in serum supplemented media with 1nM E2 for one week in 12 wells. Data are representative of the mean + SEM relative to each cell line's vehicle control ($n \geq 3$, ***$P \leq 0.001$, 2-way ANOVA followed by Bonferroni multiple comparison test). *ESR1* mutant cell lines are averages of two independent clones.

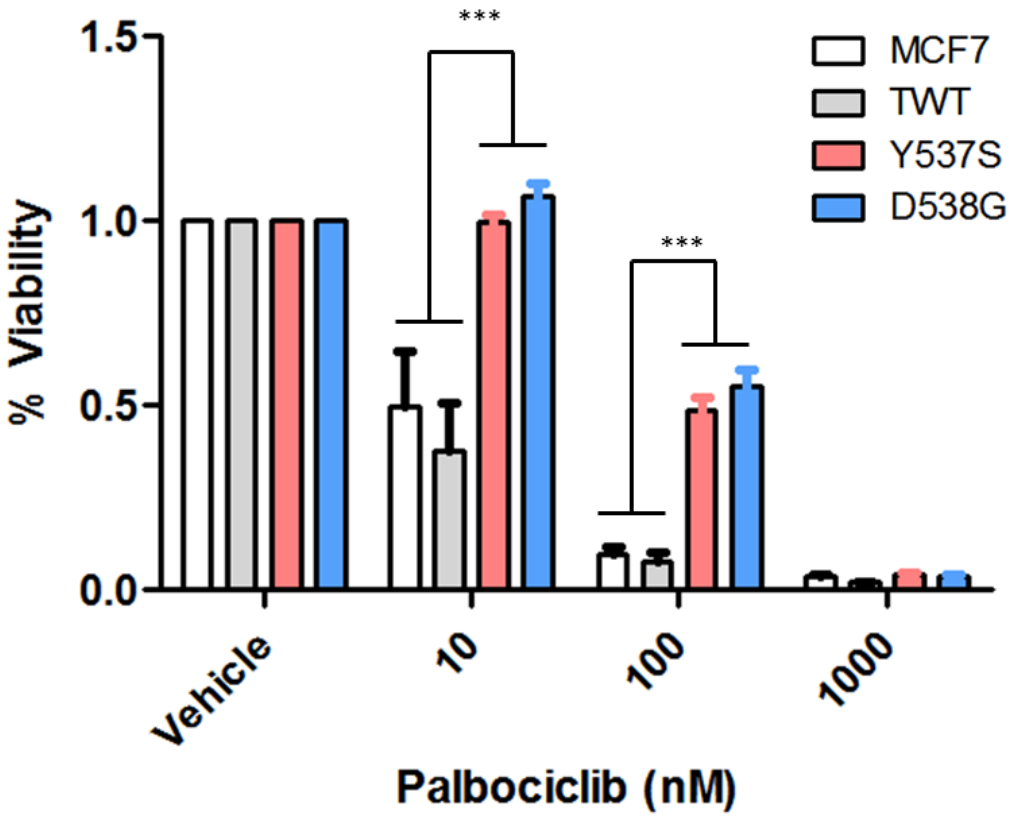

Figure 2.8: MCF7, MCF7 TWT and MCF7 *ESR1* mutants treated with palbociclib in serum supplemented media with 1nM E2 for one week in 12 wells. Data are representative of the mean + SEM relative to each cell line's vehicle control ($n \geq 3$, $^{***}P \leq 0.001$, 2-way ANOVA followed by Bonferroni multiple comparison test). *ESR1* mutant cell lines are averages of two independent clones.

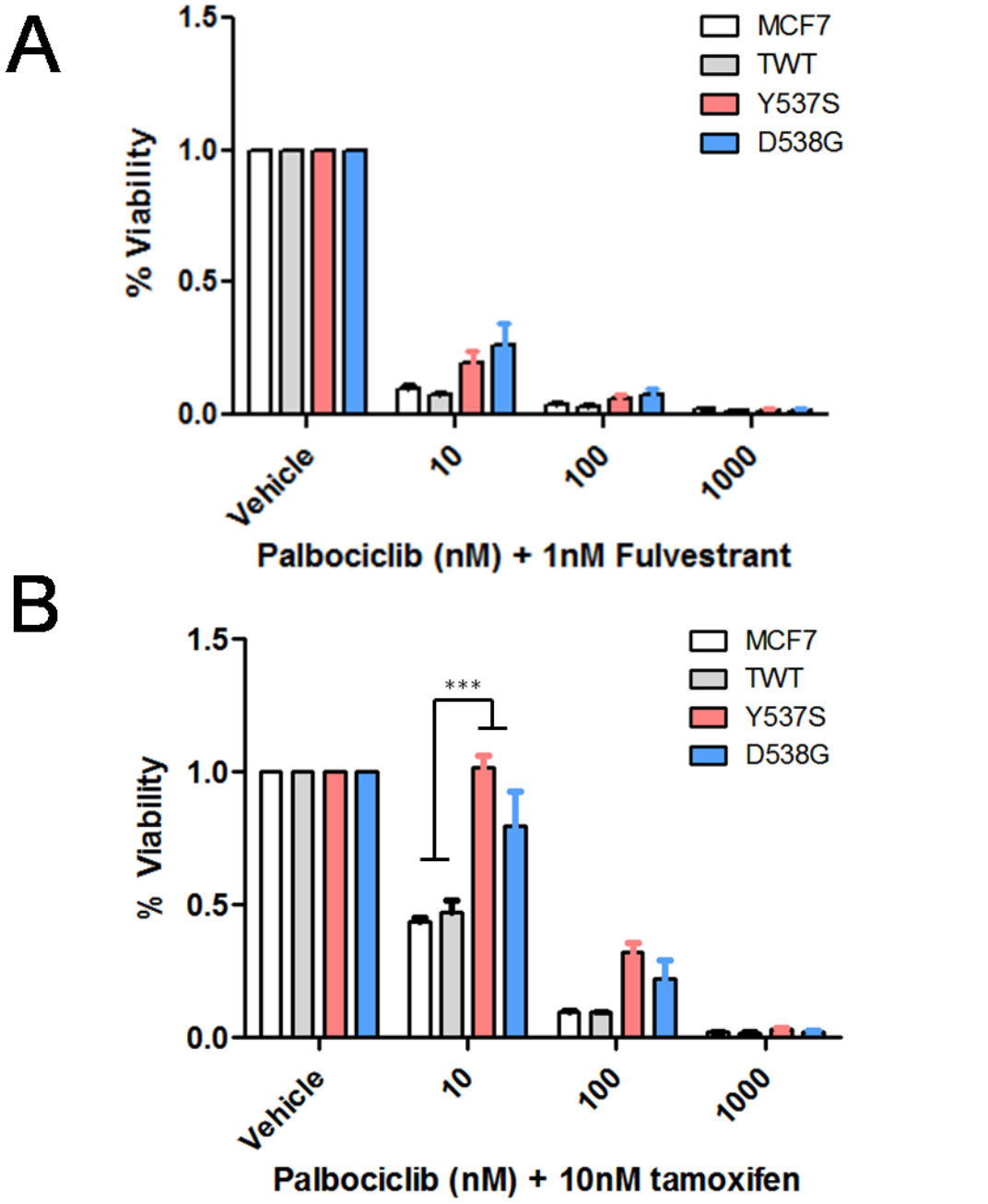

Figure 2.9: MCF7, MCF7 TWT and MCF7 *ESR1* mutants treated with palbociclib in serum supplemented media with 1nM E2 and 10nM fulvestrant (A) or 10nM tamoxifen (B) for one week in 12 wells. Data are representative of the mean + SEM relative to each cell line's vehicle control ($n \geq 3$, $^{***}P \leq 0.001$, 2-way ANOVA followed by Bonferroni multiple comparison test). *ESR1* mutant cell lines are averages of two independent clones.

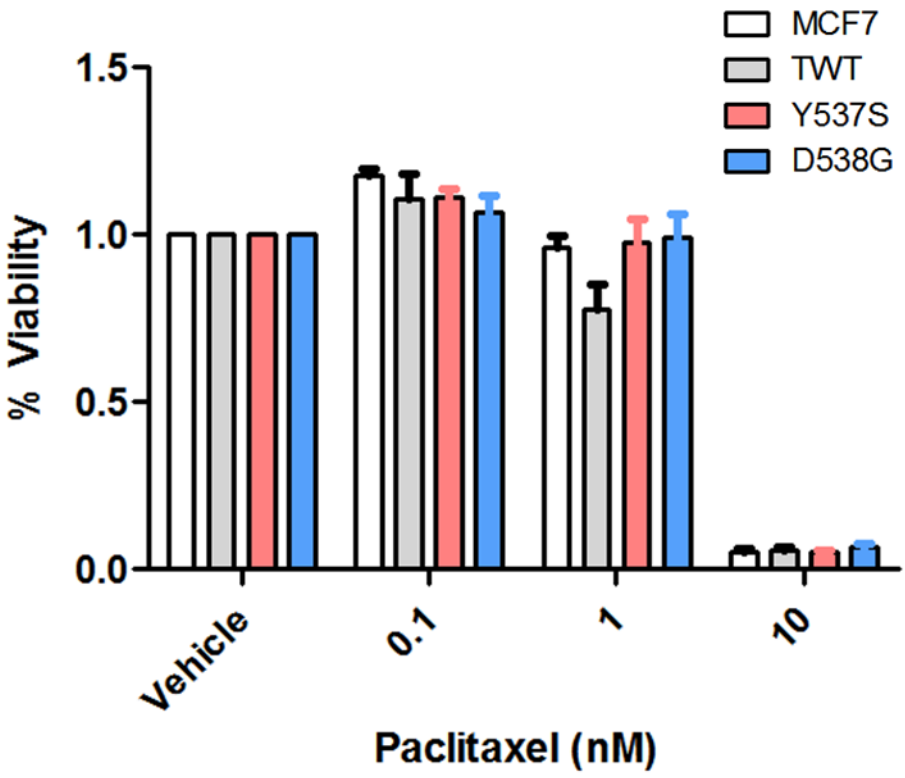

Figure 2.10: MCF7, MCF7 TWT and MCF7 *ESR1* mutants treated with paclitaxel in serum supplemented media with 1nM E2 for one week in 12 wells. Data are representative of the mean + SEM relative to each cell line's vehicle control (n ≥ 3). *ESR1* mutant cell lines are averages of two independent clones.

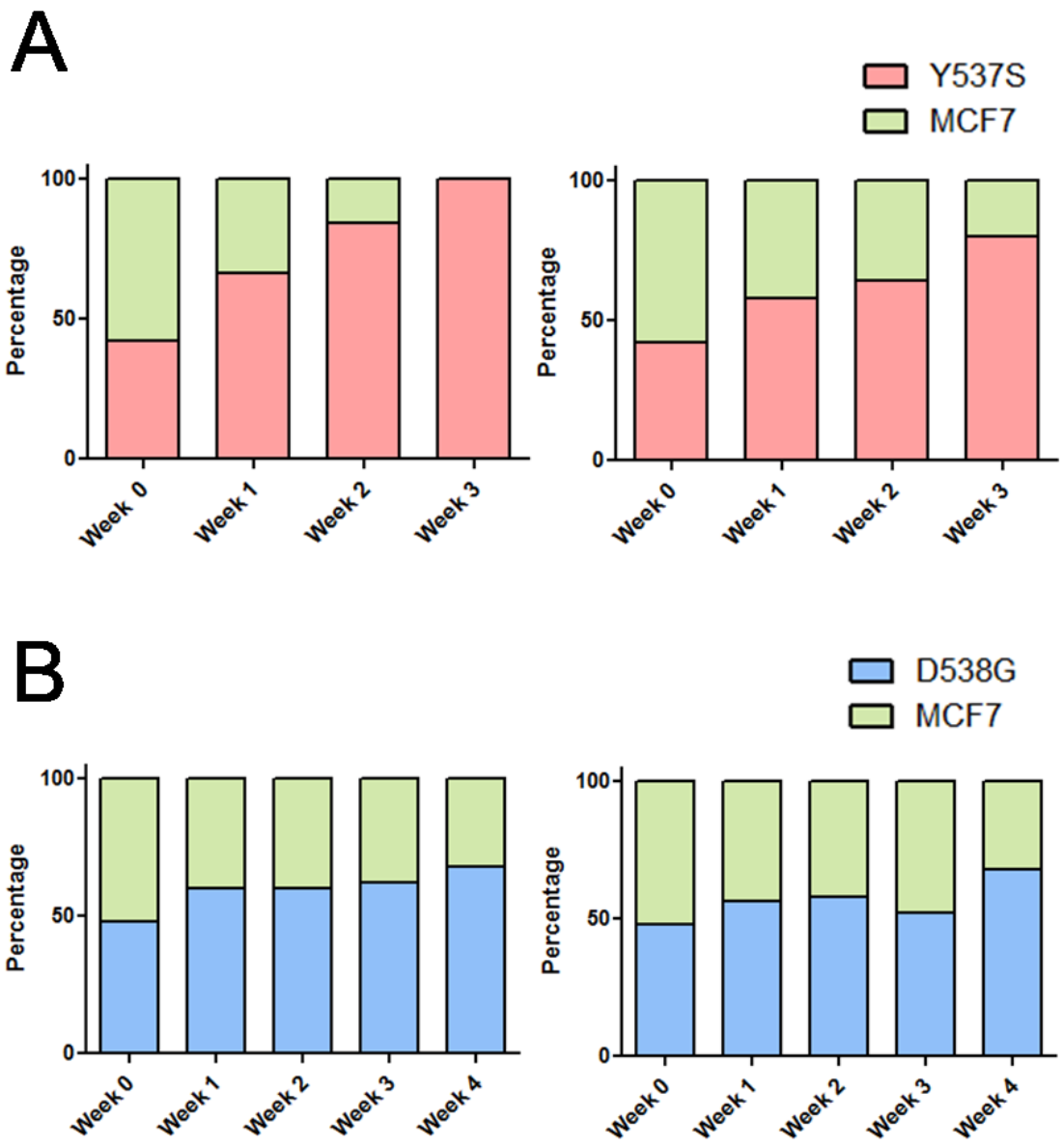

Figure 2.11: MCF7 parental and MCF7 *ESR1* Y537S (A) and D538G (B) mutants were co-cultured in serum supplemented with 1nM E2 and 10nM tamoxifen (left) or 1nM fulvestrant (right). Genomic DNA was isolated every 7 days and analyzed via ddPCR. Bars represent the ratio of MCF7 parentals to MCF7 *ESR1* mutants.

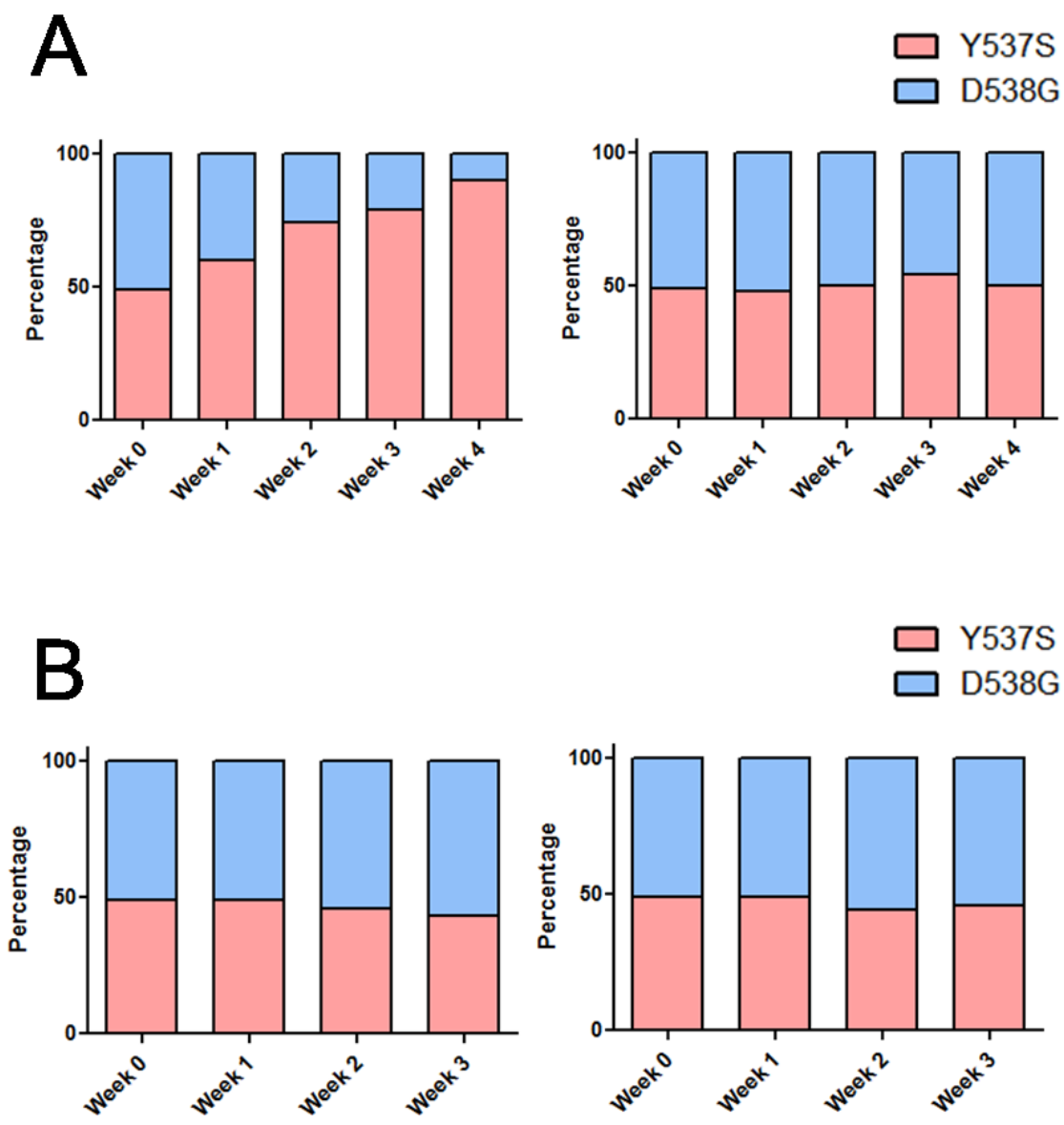

Figure 2.12: MCF7 *ESR1* Y537S and D538G were co-cultured (A) or single cultured (B) in serum supplemented (left column) and serum supplemented media with 1nM E2 (right column). Genomic DNA was isolated every 7 days and analyzed via ddPCR. Bars represent the ratio of MCF7 *ESR1* Y537S to MCF7 *ESR1* D538G. Two independent experiments were performed.

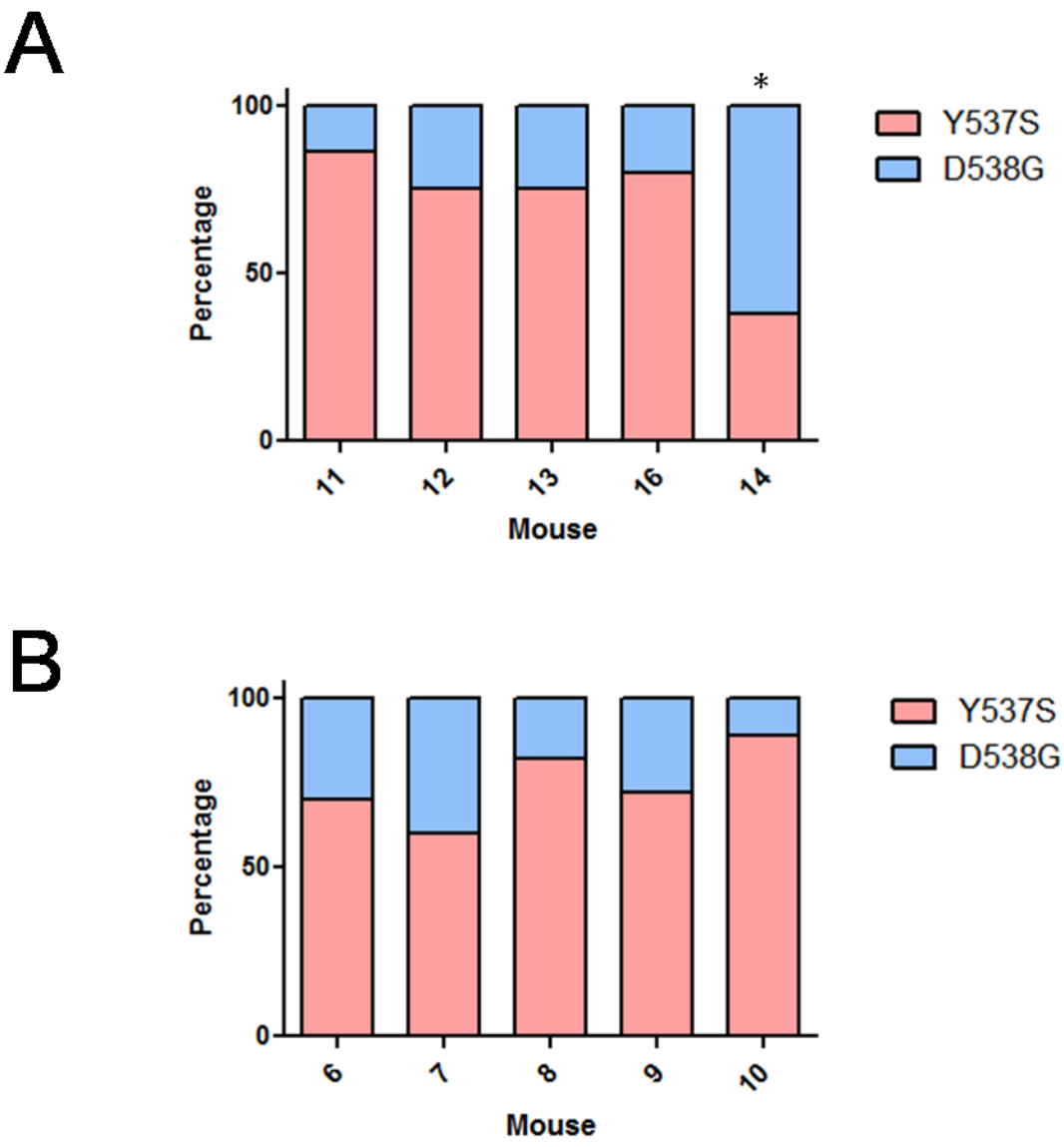

Figure 2.13: MCF7 *ESR1* Y537S and D538G cells were co-inoculated in mice with (A) and without (B) E2 pellet supplementation. Tumors were harvested when volumes reached approximately 300mm^3. Genomic DNA was isolated and analyzed via ddPCR. Bars represent the ratio of MCF7 *ESR1* Y537S to MCF7 *ESR1* D538G. *Mouse 14 did not demonstrate any tumor growth.

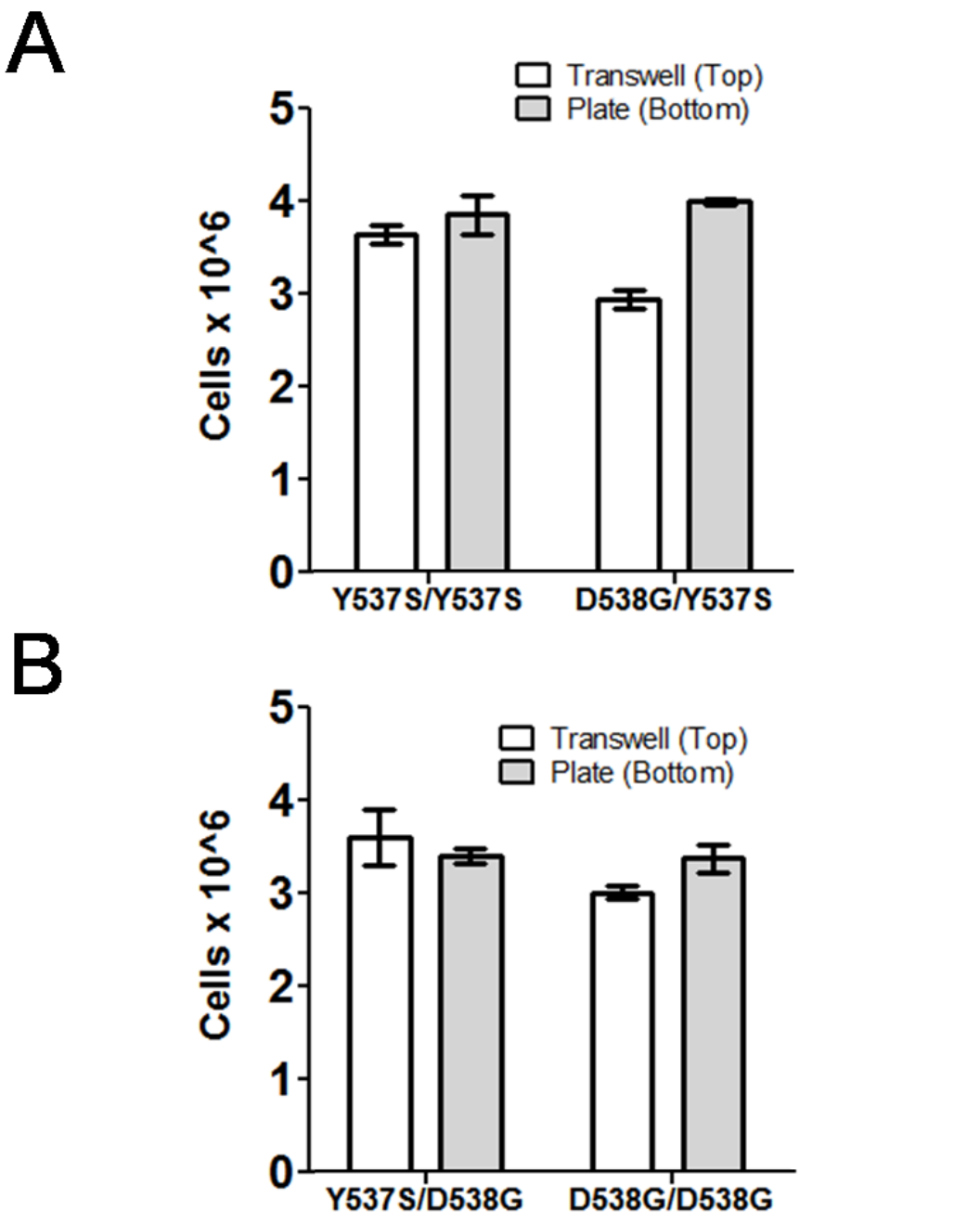

Figure 2.14: MCF7 *ESR1* Y537S and D538G cells were plated on transwells inserts with MCF7 *ESR1* Y537S cells (A) or MCF7 *ESR1* D538G cells (B) plated on 6 wells in serum supplemented media. Cells were grown together for 13 days and cell counted. Data are representative of the mean+SEM (n ≥ 3). Two independent experiments were performed.

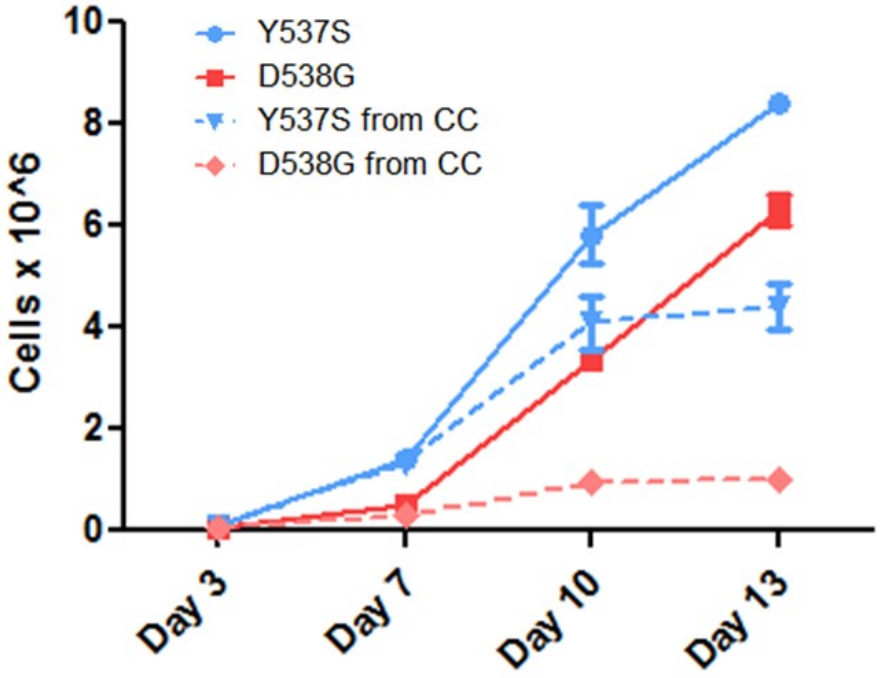

Figure 2.15: MCF7 *ESR1* Y537S and D538G were cultured singly or in co-cultures (CC) in serum supplemented media. Cells were counted and genomic DNA was isolated at the indicated time points. The amount of MCF7 *ESR1* Y537S and D538G cells present in co-cultured was obtained via ddPCR. Data are representative of the mean+SEM (n ≥ 3). Two independent experiments were performed.

Table 2.1: Cell lines used in this study

Cell Line	Description
MCF7	Parental MCF7 cell line
MCF7 *ESR1* Y537S	MCF7 with single *ESR1* Y537S knock in allele
MCF7 *ESR1* D538G	MCF7 with single *ESR1* D538G knock in allele
MCF7 Targeted WT	MCF7 with wild type vector knock in allele

Table 2.2: Homology Arm Cloning Primers

Locus	Homology Arm	Forward/Reverse Primer
ESR1 exon 10	5'	5'-GCAGAGTTGTGGCTAGTGGA
		5'-AAGCTGAGGGCTTTCAGAAG
	3'	5'-TCCCAGCTCCCATCCTAAAGTG
		5'-AAAGGATGCATTGCCATAGG

Table 2.3: Mutagenesis Primers

Locus	Mutant	Forward/Reverse Primer
ESR1 exon 10	Y537S	5'-CCTCTcTGACCTGCTGCTGGA
		5'-TCCAGCAGCAGGTCAgAGAGG
	D538G	5'-CCTCTATGgCCTGCTGCTGGA
		5'-TCCAGCAGCAGGcCATAGAGG

Table 2.4: Pre-Cre Screening Primers

Locus	Homology Arm	Forward/Reverse Primer
ESR1 exon 10	5'	5'-GGCAAGTCTCCAACTTGAGC
		5'-GCAGACAGCGAATTAATTCC
	3'	5'-TTAAGGTACCACTGTGCATATG
		5'-CCGGGAAGATCCAAGTACAG

Table 2.5: Post-Cre Screening Primers

Locus	Forward/Reverse Primer
ESR1 exon 10	5'-GGCAAGTCTCCAACTTGAGC
	5'-CATATGCACAGTGGTACCTTAA

Table 2.6: Bi-Allelic Sequencing Primers

Locus	Forward/Reverse Primer	Forward/Reverse Primer
ESR1 exon 10	5'-TCCCAGCTCCCATCCTAAAGTG 5'-AAAGGATGCATTGCCATAGG	5'-CCCCTTCTAGGGATTTCAGC

Table 2.7: Targeted Allele Sequencing Primers

Locus	Forward/Reverse Primer	Forward/Reverse Primer
ESR1 exon 10	5'-TTAAGGTACCACTGTGCATATG 5'-AGAGGCAGAGCTTTCAGCAC	5'-TCCCAGCTCCCATCCTAAAGTG

Table 2.8: cDNA Sequencing Primers

Locus	Forward/Reverse Primer	Forward/Reverse Primer
ESR1 exon 10	5'-TGGAGATCTTCGACATGCTG 5'-ATGAAGTAGAGCCCGCAGTG	5'-GCACCCTGAAGTCTCTGGAA

Table 2.9: ddPCR Primers

Locus	Forward/Reverse Primer
ESR1 exon 10	5'-GCATGAAGTGCAAGAACGTG
	5'-AGACGGACCAAAGCCACTT

Table 2.10: ddPCR Probes

Mutation	Sequence
ESR1 Y537S	5'-TCTcTGACCTGCTGCTGGAGATGCT
ESR1 Y537N	5'-TCaATGACCTGCTGCTGGAGATGCT
ESR1 D538G	5'-TCTATGgCCTGCTGCTGGAGATGCT
ESR1 WT	5'-TCTATGACCTGCTGCTGGAGATGCT

3 Detection of *ESR1* mutations in circulating plasma tumor DNA from metastatic breast cancer patients

*This work has been published and reprinted here.

Chu D, Paoletti C, Gersch C, VanDenBerg DA, Zabransky DJ, Cochran RL, Wong HY, Toro PV, Cidado J, Croessmann S, Erlanger B, Cravero K, Kyker-Snowman K, Button B, Parsons HA, Dalton WB, Gillani R, Medford A, Aung K, Tokudome N, Chinnaiyan AM, Schott A, Robinson D, Jacks KS, Lauring J, Hurley PJ, Hayes DF, Rae JM, Park BH. *ESR1* Mutations in Circulating Plasma Tumor DNA from Metastatic Breast Cancer Patients Clin Cancer Res February 15 2016 (22) (4) 993-999; DOI: 10.1158/1078-0432.CCR-15-0943

Introduction

Our ability to adequately treat and manage disease hinges on an accurate and proper diagnosis. Historically, tissue biopsies have been the gold standard in oncology, providing histopathological information on whether or not a lesion is

malignant. In addition to determining whether a lesion may be malignant, tissue biopsies provide a reservoir for genetic information. In a seminal study, Wood *et al*. utilized Sanger sequencing to unravel the range and frequencies of genetic alterations that make up breast and colorectal tumors, now known as the "cancer genome landscape"[46]. The hope is that this genetic information can reveal what genes might be altered or disrupted that promote cancer, namely "drivers," and how these alterations can be targeted.

However, despite their utility, there are challenges to acquiring tissue biopsies and how they are processed for subsequent analysis. Obtaining biopsies is inherently invasive and depending on the stage of the disease and the amount of tissue isolated, can be limiting in quantity for genomic analysis. Most tumor tissues are subsequently preserved in formalin-fixed, paraffin-embedded (FFPE) blocks for pathological interpretation and staining. However, this process crosslinks and fragments DNA, jeopardizing their structural integrity and introduces challenges for sequencing and interrogating genomic alterations. Lastly, cancer is an inherently heterogeneous disease, where different areas of the same tumor or different metastases can arise from different subclonal populations, namely intra- and intertumoral heterogeneity, respectively. Biopsying a single site provides only a single spatial and temporal snapshot and unlikely to reflect the dynamic tumor heterogeneity in patients[72].

In light of this, development of noninvasive techniques such as liquid biopsies as a surrogate for tissue biopsies has garnered increased interest. Compared to tumor biopsies, blood draws are minimally invasive and provide a

source of cell free DNA (cfDNA) for serial sampling to monitoring disease. Cell free DNA is derived from all cells, including both normal and cancers cells, with the latter more commonly referred to as circulating tumor DNA. Since the DNA of cancer cells harbors somatic alterations, that is, mutations, amplifications and rearrangements not present in normal cells, cancer DNA presents a unique "fingerprint" that can be used to differentiate cancer from non-cancerous cells. Indeed, studies have demonstrated that the mutational profile generated from analyzing ctDNA generally reflects the same somatic alterations found in patients' cancers, and can sometimes capture mutations not present in the initial biopsy[73-74].

The identification of *ESR1* mutations that are responsible for endocrine therapy resistance in ER-positive breast cancers opens the door for developing new diagnostic tools and novel targeted therapies[6-8, 10, 75]. However, given the problem of tumor heterogeneity, the true frequency of *ESR1* mutations may be underestimated, since mutational profiles can vary between different sites of metastatic disease[72]. Most studies heretofore have employed NGS of a single metastatic site, and indeed, one study demonstrated an *ESR1* mutation in a liver metastatic biopsy but not a lung metastasis obtained from the same patient[10]. Further, in many cases, fresh biopsies of metastatic disease cannot be safely obtained and/or archival tissues are inadequate or unavailable. Finally, these mutations appear to evolve during endocrine treatment, and therefore a non-invasive method of monitoring patients might provide an opportunity to alter therapy as these mutations emerge. Thus, there is need to develop non-invasive

methods to quickly assess mutational profiles across multiple metastases from an individual patient.

Recently, we and others have examined the use of circulating cell-free plasma tumor DNA (ptDNA) as a biomarker for cancer detection[76-83]. It is known that DNA molecules from both normal and cancer cells are shed or released into the circulation[84-85]. Because DNA from cancer cells harbor somatic mutations and rearrangements, these can serve as specific genetic biomarkers for the presence of cancer. Further, the quantity of ptDNA directly correlates with tumor burden and response to therapies[86]. Additionally, several groups have demonstrated the ability to detect the presence of acquired drug resistance mutations in ptDNA[87-88], which opens the possibility for earlier therapeutic intervention. More recently, our group has shown that a next generation digital PCR platform, termed droplet digital PCR (ddPCR) has exquisite sensitivity and specificity for detecting cancer mutations in early stage breast cancer patients[82]. We hypothesized that ddPCR could be a more sensitive platform for *ESR1* mutation detection in metastatic breast cancer patients and may show a more accurate frequency of these mutations in ER-positive disease. To test this hypothesis, we performed ddPCR for *ESR1* mutations on cell-free plasma samples from patients with metastatic breast cancer and compared *ESR1* mutations in ptDNA with NGS of metastatic tumor tissue from the same patients.

Results

We enrolled a total of 23 patients in two separate cohorts (Figure 3.1) from UMCCC and JHSKCCC. Systemic endocrine therapies are shown (Table 3.1), though many patients also received prior chemotherapies. To determine if we could identify circulating *ESR1* mutations in patients with known tissue *ESR1* status, we initially performed a retrospective analysis by obtaining plasma samples from eleven patients who had previously undergone NGS of a metastatic lesion (Table 3.2). Plasma DNA was obtained from these patients less than 1 year after their tissue biopsy (median = 145 days, range 54 to 344 days). Eight of these patients (patients 1-8) had *ESR1* mutations identified via NGS in their metastatic biopsies, and three patients (patients 9-11) had wild type *ESR1*. Patients 1- 3 had previously been reported as having an *ESR1* tissue mutation[8] identified via the MiONCOSEQ program at UMCCC[89], while patients 4-8 had *ESR1* mutations identified at JHSKCCC using a commercial platform (Foundation Medicine). All patients had documented ER-positive disease, and NGS was performed on samples representing diverse metastatic sites (Table 3.1). The plasma specimens were interrogated for all three *ESR1* hotspot mutations: Y537S, Y537N and D538G, using mutation specific probes and ddPCR as previously reported[82]. These three mutations were chosen as they collectively represent the most frequent *ESR1* mutations in metastatic disease[75]. As demonstrated in Figure 3.2, each probe was specific for its respective mutation using Y537S, Y537N and D538G mutant and wild type templates. As shown in Table 3.2, ddPCR successfully detected all mutations in ptDNA that

were detected in the metastatic biopsy, confirming the ability to detect mutations present within the tumor sample. The majority of patients had significant tumor burden with multiple metastatic sites of disease (Table 3.4), though patient 5 had no evidence of disease after removal of her metastatic lesion. Indeed, although she did have a circulating *ESR1* mutation (D538G), it was detected at a relatively low fractional abundance (0.03%) in her plasma.

In addition to harboring the known tissue mutation (Y537S in her circulation), patient 1 also had a low fractional abundance (0.01%) of a second circulating mutation, D538G, which was not detected in the metastatic tissue. It should be noted, however, that her blood was drawn 186 days after biopsy, and thus a new subclonal population within the same metastatic site could have been present at the time of blood draw. Similarly, patient 9 was wild type for *ESR1* in the metastatic lesion but showed a D538G mutation at a relatively low fractional abundance in a plasma sample obtained 54 days after biopsy. These results suggest that ddPCR of ptDNA can reliably detect *ESR1* mutations first identified in metastatic tissues and may also detect subclonal populations in the metastatic biopsy below the limit of detection by NGS, or mutations from other sites of disease.

The presence of two additional mutations in patients 1 and 9 may have been due to clonal evolution in the interim between tissue biopsy and blood draw for ptDNA analysis. To address this possibility, we prospectively enrolled eight additional ER-positive patients (patients 12-19) to simultaneously collect metastatic tissue biopsies and blood for NGS and ddPCR analysis, respectively.

As controls, we also obtained metastatic tissue and blood samples from four ER-negative patients (patients 20-23). All patients were enrolled at UMCCC except patient 19 who was enrolled at JHSKCCC. As shown in Table 3.3, sufficient tissue could not be obtained for patients 12 and 19, while patient 14 did not have adequate sample for NGS analysis. These patients highlight the fact that metastatic biopsies are not always obtainable and that the amount of tissue can preclude genomic analysis.

After plasma DNA extraction, ddPCR analysis was performed in a blinded fashion. As seen in Table 3.3, all patients had blood drawn at the time of tissue biopsy, except two patients (patients 20 and 21) had blood drawn 5 and 3 days after biopsy, respectively, for logistical reasons. Of the five ER positive patients for whom tissue NGS results could be obtained, no *ESR1* mutations were identified in their metastatic biopsies. However, *ESR1* mutations were detected in the ptDNA samples from three of these patients (patients 13, 16, and 18), all of whom had their blood drawn the same day as biopsy. Of note, patient 16 was a known germline *BRCA2* mutation carrier and may have had a primary peritoneal (ovarian) carcinoma concurrent with her liver metastases, thus obfuscating the origin of the liver lesion. As expected, the ER-negative patients (patients 20-23) did not have detectable *ESR1* mutations in their ptDNA. The difference in mutational status was statistically significant between tissue and blood using two-tailed Fisher's exact test ($p<0.0186$).

Interestingly, patient 14, who was ER-positive, had a high fractional abundance of two distinct circulating *ESR1* mutations (Y537S, 5.02%; D538G,

2.62%). Her only metastatic site amenable to biopsy was a pleural effusion, which was inadequate for NGS. The ptDNA from this patient collected concurrently at the time of biopsy contained two distinct mutations at differing allelic frequencies, suggestive of two separate clonal populations. This was similar to patient 1, and suggestive that the mutations were on separate alleles. To prove this, we developed a dual mutation specific probe and positive control template. As shown in Figure 3.3, this probe has specificity for a synthetic allele harboring both mutations. Analysis of ptDNA from patients 1 and 14 using this probe showed no positive signals, demonstrating that the two *ESR1* mutations are on separate alleles, further supporting that these *ESR1* mutations are derived from different clonal populations.

An additional noteworthy case is patient 19, who presented at the time of diagnosis with wide spread, bone only ER-positive metastatic disease. She initiated treatment with the AI letrozole, and after 1 year of therapy restaging scans showed disease stabilization of her bony metastasis, and complete resolution of her breast tumor. She elected to have bilateral mastectomies, which revealed that the affected breast and the contralateral breast had no evidence of disease. She remained on letrozole for 5 years with stable disease. She enrolled in our study while still in remission, although restaging scans continued to demonstrate only prior bony lesions, which were not amenable to biopsy. Nonetheless, her plasma demonstrated the presence of the Y537N mutation. Because of her unusual presentation, this is the only patient in our cohort that had developed an *ESR1* mutation after exposure to a single

endocrine therapy, letrozole. Subsequently, she had an asymptomatic elevation in her tumor markers and her therapy was changed to fulvestrant. Clinically she remains without evidence of progression and has had stabilization of tumor markers. Although other studies have suggested that AIs may be the class of endocrine therapies that selects for LBD *ESR1* mutations[90], most studies have enrolled patients who have received multiple lines of endocrine therapy in both the adjuvant and metastatic settings, which precludes any definitive conclusions. This patient demonstrates that an *ESR1* mutation can indeed occur after prolonged exposure to an AI without other endocrine or systemic therapies, and that *ESR1* mutations do not necessarily preclude response to a subsequent fulvestrant.

Discussion

There are several important conclusions with potential therapeutic implications derived from our study. First, we have demonstrated that *ESR1* mutations can be readily detected using ddPCR on plasma from patients with metastatic ER-positive disease after progression on endocrine therapies. Given challenges that can arise in obtaining a metastatic biopsy as encountered in this study, the use of ptDNA as a “liquid biopsy” holds great promise for future molecular analysis of human cancers. Moreover, monitoring for emergence of mutated clones by repeat sampling can be more easily performed with a simple blood test than with multiple tissue biopsies. Second, we demonstrate that blood can be a more sensitive source for detecting *ESR1* mutations. In our study two

patients harbored a distinct, second *ESR1* mutation not present in the corresponding metastatic biopsies. Perhaps more importantly, one patient in cohort 1 and three patients in cohort 2 had wild type *ESR1* in their metastatic biopsies, but had *ESR1* mutations detected in their corresponding ptDNA sample. These results support the increasingly recognized problem of tumor heterogeneity and are in agreement with a prior report demonstrating differences in *ESR1* mutation status between two metastatic sites within the same patient[10]. Third, our results support the previously proposed hypothesis that *ESR1* LBD mutations may be selected for after progression on AIs[8]. This was particularly striking in patient 19, who was positive for an *ESR1* mutation and had received only prolonged exposure to letrozole. Fourth, our study shows that ddPCR of ptDNA is capable of detecting *ESR1* mutations even in patients who have no radiographic evidence of disease. Although the clinical validity and utility of this observation remains to be proven, we suggest that detecting drug resistant mutations may afford the opportunity to change therapies earlier or enroll in trials of novel targeted therapies, which may lead to improved outcomes for patients. Finally, the frequency of circulating *ESR1* mutations in our study is notably higher than prior reports using a single metastatic biopsy. The majority of studies thus far have detected *ESR1* mutations only in patients with metastatic disease after progression on endocrine therapies, though one study did find a low incidence (3%) in primary tumors[7]. The largest study to date of *ESR1* mutations in metastatic tissue biopsies suggests an overall frequency of 12%, with a frequency of 20% in a subgroup analysis of patients who received an average of

7 lines of therapy[75]. However, we found additional mutations not detected by sequencing of metastatic lesions. In cohort 1, two additional mutations were discovered: patient 1 who had an additional *ESR1* mutation found in ptDNA compared to her metastatic biopsy, and patient 9 who was wild type for *ESR1* on her metastatic tissue sample. Additionally, in cohort 2, we detected seven *ESR1* mutations in six of the eight ER-positive patients not detected in metastatic biopsies, although three of these patients did not have adequate tissue for NGS. These results highlight the potential impact of using blood as a more sensitive and accessible source for mutation detection.

The higher frequency of *ESR1* mutations in blood compared to biopsied tissues could be due to several non-overlapping reasons. As mentioned, tumor heterogeneity can lead to the detection of mutations in ptDNA that are present in other non-biopsied metastatic sites. It is also conceivable that sampling error of biopsies may miss subclonal populations in a given metastatic lesion, and/or certain clonal populations may have a propensity for releasing ptDNA versus other clonal variants. For example, it is possible that ptDNA shed from CTCs is more abundant than ptDNA derived from other metastatic sites. Further studies are needed to clarify the origins and kinetics of ptDNA as related to sites of metastases, and any underlying biology that may favor the enrichment of clonal populations that shed higher versus lower amounts of ptDNA into the circulation.

There are limitations of our study, most notably the small sample size, which prevents our assessing the true prevalence of *ESR1* mutations in plasma from patients with ER-positive breast cancer. Further, we only queried for the

three most common *ESR1* LBD mutations, and it is likely ptDNA contains other *ESR1* mutations associated with endocrine therapy resistance. Although additional *ESR1* LBD mutations have been described at lower frequency[6-8, 10, 75], we did not identify these mutations by NGS of tissues in the retrospective cohort, and they were therefore not queried by ddPCR. In addition, because these mutations are all in close proximity to one another, each *ESR1* ddPCR mutation probe was run separately due to potential competition for the same template molecule, which could theoretically decrease the sensitivity for any given probe. This can limit the number of mutations that can be assayed due to low amounts of plasma DNA. However, this limitation may have led us to underestimate the prevalence of *ESR1* mutations in our study.

In summary, we confirm the feasibility of detecting *ESR1* mutations in ptDNA, and that plasma may prove to be a superior source than metastatic biopsies for *ESR1* mutation detection. However, the clinical utility of using ddPCR for *ESR1* mutations to guide therapy for patients requires careful prospective study before adoption into clinical practice. It is unknown what allelic frequency of *ESR1* mutation is associated with symptomatic disease progression, and whether changing endocrine therapies can improve patient outcomes. Nevertheless, the ability to detect *ESR1* mutations in the plasma of patients, independent of the tissue mutational status, provides the foundation for future clinical trials to track and monitor the emergence of endocrine therapy resistance.

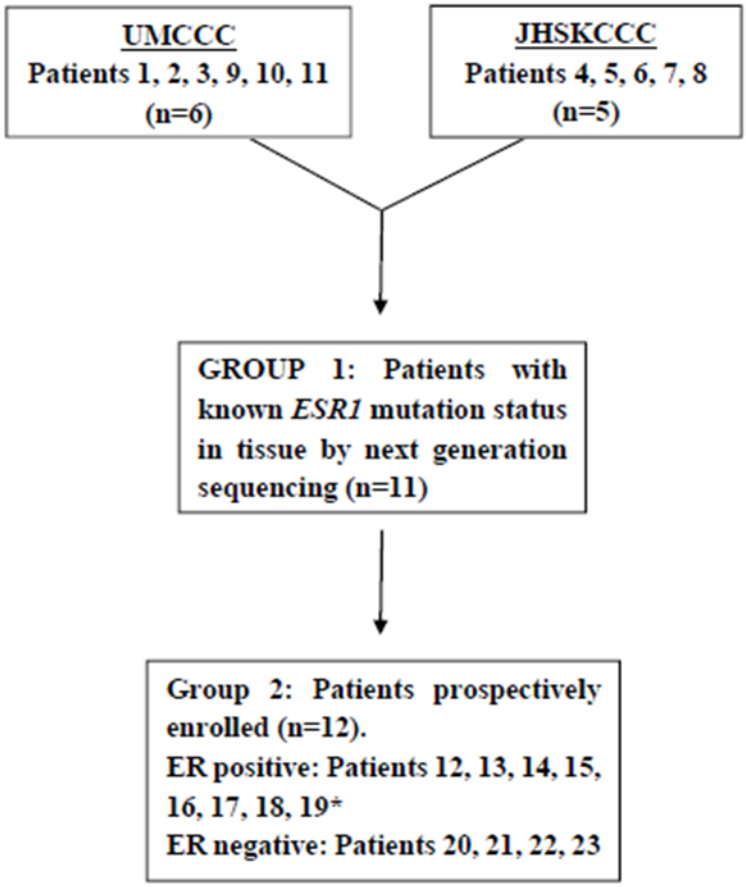

Figure 3.1: Patient enrollment and distribution. Cohort 1: Patients were enrolled retrospectively after next generation sequencing of a metastatic biopsy at UMCCC and JHSKCCC (cohort 1) confirming the presence of an *ESR1* mutation (patients 1, 2, 3, 4, 5, 6, 7, 8, 9), or wild type *ESR1* (patients 10, 11, 12), with blood obtained after tissue sequencing was performed for ddPCR. Cohort 2: Patients were enrolled prospectively, with tissue and blood obtained contemporaneously. Tissue was subjected to next generation sequencing and blood was analyzed by ddPCR, with sequencing results blinded to ddPCR investigators. *All cohort 2 patients were enrolled at UMCCC except patient 19.

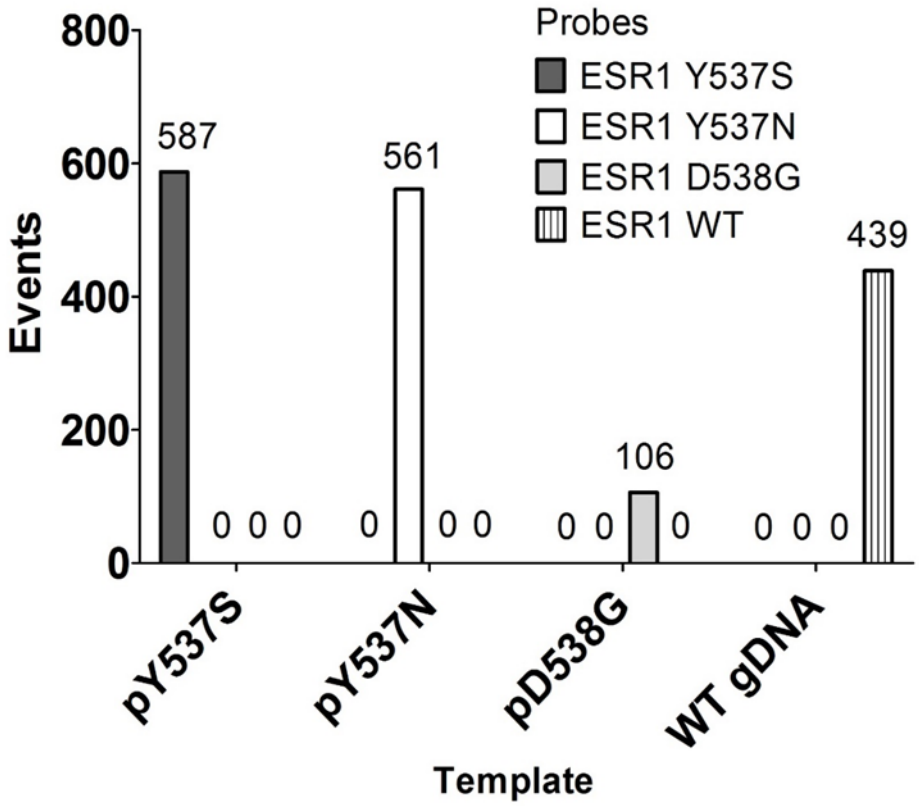

Figure 3.2: Plasmids containing a single *ESR1* mutation (pY537S, pY537N and pD538G) and wild type genomic DNA (WT gDNA) were assayed with *ESR1* Y537S, *ESR1* Y537N, *ESR1* D538G or *ESR1* WT probes using ddPCR. The number of positive events, or genomic equivalents, is shown as the sum of two samples.

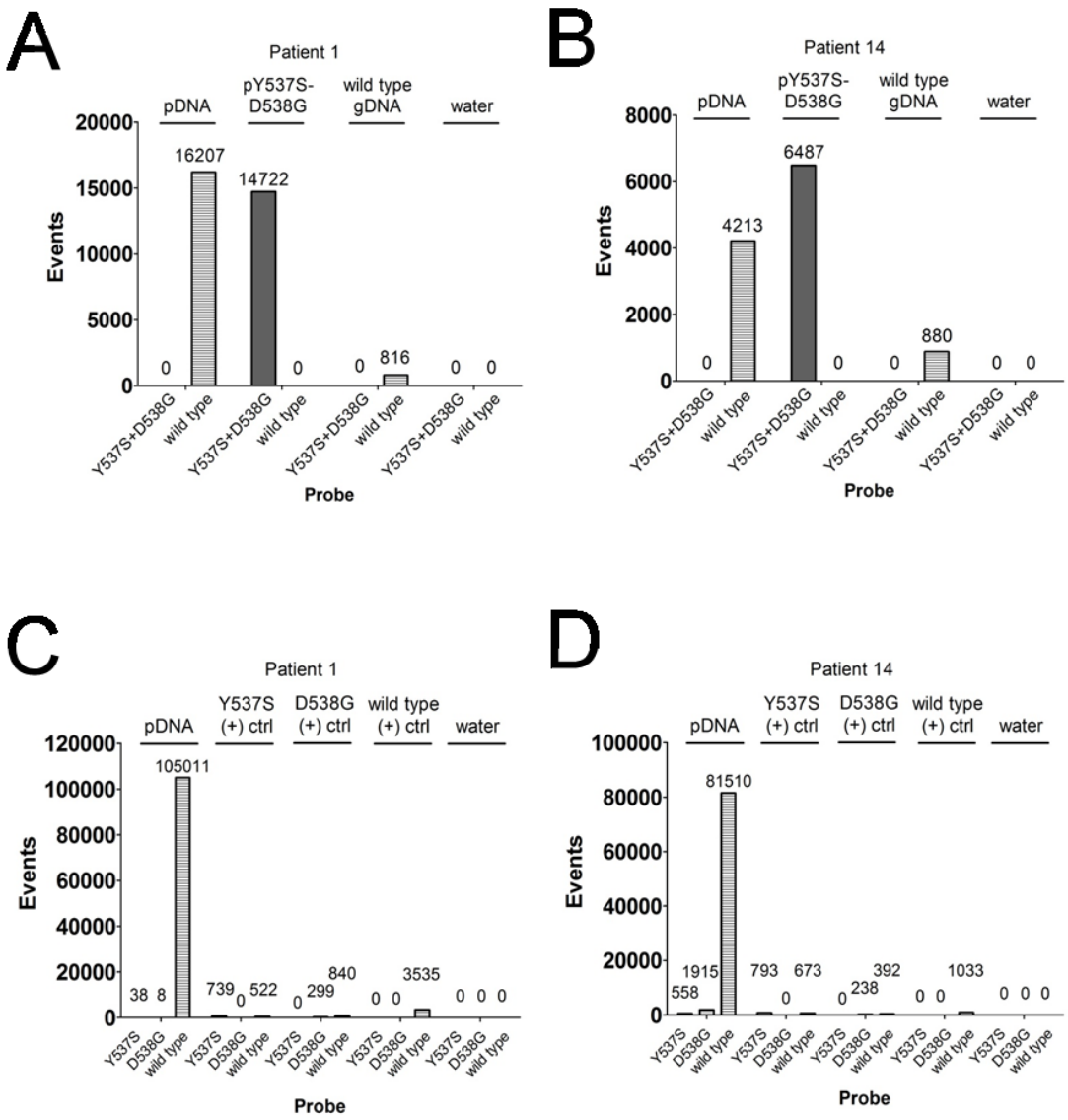

Figure 3.3: Patients 1 and 14 plasma DNA (pDNA), synthetic template (pY537S+D538G) and various controls were assayed with a dual mutant *ESR1* Y537S+D538G and *ESR1* wild type probe using ddPCR (A and B). Additionally, the patient 1 and 14 pDNA and single mutant and wild type positive controls were assayed with single mutant *ESR1* Y537S, D538G and *ESR1* wild type probes using ddPCR. The number of positive events, or genomic equivalents, is shown as the summation of the number of wells assayed.

Table 3.1: Patient characteristics

Patient	Age at study entry (median = 58)	Site of tissue biopsy	Primary ER/PR/HER2	Metastatic ER/PR/HER2	Treatment
Cohort 1					
1	58	Peritoneal fluid	+/+/-	+/+/-	Tamoxifen x 5 years (adjuvant), letrozole (metastatic), tamoxifen (metastatic), fulvestrant, exemestane + everolimus
2	45	Liver	+/+/-	+/+/-	Tamoxifen x 4 years (adjuvant), anastrozole (metastatic), fulvestrant, estrace, exemestane
3	60	Liver	+/+/-	+/+/+	Tamoxifen x 5 years (adjuvant), letrozole (metastatic)
4	56	Liver	NA	+/+/-	Tamoxifen and zolendronic acid x 4 years, anastrozole x 6 weeks, fulvestrant x 1 year, exemestane x 2 months
5	37	Liver	+/-/-	+/-/-	Tamoxifen x 2 year (adjuvant), letrozole (+sorafenib on trial) x 4 months, anastrozole x 1 year, fulvestrant x 4months
6	63	Brain	+/+/NA	+/+/-	Tamoxifen x 1 year, letrozole x 1 year, fulvestrant x 6 months
7	70	Liver	+/+/NA	+/+/-	Tamoxifen (adjuvant), letrozole, exemestane + everolimus, fulvestrant (many years)
8	65	Liver	+/+/NA	+/+/-	Tamoxifen x 5 years (adjuvant), letrozole x 5 years (adjuvant), anastrozole x 1.5 years, fulvestrant x 8 months
9	46	Sternal mass	+/+/-	+/-/-	Tamoxifen (adjuvant), anastrozole (adjuvant), anastrozole (metastatic), fulvestrant + anastrozole (metastatic)
10	67	Skin and subcutaneous tissue	+/+/-	+/+/-	Tamoxifen x 5 years (adjuvant), exemestane, fulvestrant (metastatic)
11	58	Bone	+/+/-	+/-/-	Tamoxifen x 2 years (adjuvant), anastrozole (adjuvant), fulvestrant (metastatic)
Cohort 2					
12	61	Unable to get tissue for analysis	+/NA/NA	+/+/-	Tamoxifen x 3.5 years (adjuvant), letrozole 1.5 years (adjuvant), anastrozole (adjuvant), fulvestrant + anastrozole (metastatic)
13	63	Periaortic lymp node	+/+/-	+/+/-	Tamoxifen x 3 years (adjuvant), exemestane 5 years (adjuvant), anastrozole (metastatic), anastrozole + fulvestrant, exemestane
14	48	Pleural fluid	+/+/+	NA	Tamoxifen (metastatic), fulvestrant + leuprolide, fulvestrant + anastrozole + leuprolide
15	56	Right axillary lymph node	+/-/-	+/NA/-	Letrozole + goserelin (neoadjuvant), letrozole + goserelin (adjuvant), fulvestrant (metastatic), fulvestrant + letrozole
16	77	Liver	+/+/+	+/-/-	Tamoxifen x 5 years, exemestane (adjuvant), anastrozole (adjuvant)
17	63	Axillary lymph node	+/-/-	NA	Anastrozole (metastatic), fulvestrant, tamoxifen, exemestane + everolimus
18	65	Subcutaneous chest wall nodule	+/-/-	+/-/-	Anastrozole (adjuvant), tamoxifen (adjuvant), fulvestrant (metastatic)
19	65	Unable to get tissue for analysis	+/+/-	NA	Letrozole x 5 years (metastatic), fulvestrant
20	63	Skin	-/-/+	-/-/+	None
21	41	Lung, RLL	-/-/+	-/-/+	None
22	49	Right anterior chest wall	-/-/-	-/-/-	None
23	57	Liver	-/-/-	-/-/-	None

NA = not available

Table 3.2: Cohort 1: *ESR1* mutations in metastatic tissues are present in ptDNA from blood within 1 year of biopsy. Tumor samples from 11 patients with ER-positive, metastatic breast cancer were analyzed for *ESR1* mutations using next generation sequencing (Sequencing FFPE tumor tissue) and additionally, blood samples were analyzed by ddPCR for *ESR1* Y537S, Y537N and D538G mutations. Percentage reflects the fractional abundance of mutant ESR1 (Y537S, Y537N or D538G) to total *ESR1* DNA.

Patient	Days between tissue biopsy and blood draw	Sequencing FFPE tumor tissue	ddPCR plasma for *ESR1* Y537S	ddPCR plasma for *ESR1* Y537N	ddPCR plasma for *ESR1* D538G
1	186	*ESR1* Y537S	Y537S (0.87%)	wild type	D538G (0.01%)
2	344	*ESR1* Y537S	Y537S (1.69%)	wild type	wild type
3	275	*ESR1* D538G	wild type	wild type	D538G (1.55%)
4	68	*ESR1* Y537S	Y537S (0.63%)	wild type	wild type
5	64	*ESR1* D538G	wild type	wild type	D538G (0.03%)
6	165	*ESR1* D538G	wild type	wild type	D538G (4.23%)
7	88	*ESR1* D538G	wild type	wild type	D538G (0.01%)
8	60	*ESR1* Y537N	wild type	Y537N (0.68%)	wild type
9	54	wild type	wild type	wild type	D538G (0.01%)
10	145	wild type	wild type	wild type	wild type
11	270	wild type	wild type	wild type	wild type

Table 3.3: Cohort 2: *ESR1* mutations are present in ptDNA in patients with wild type ESR1 metastatic biopsies when obtained contemporaneously. Tumor samples from 8 and 4 patients with ER-positive and ER-negative metastatic breast cancer, respectively, were analyzed for *ESR1* mutations using next generation sequencing (Sequencing FFPE tumor tissue) and additionally, blood samples were analyzed by ddPCR for *ESR1* Y537S, Y537N and D538G mutations. Percentage reflects the fractional abundance of mutant ESR1 (Y537S, Y537N or D538G) to total *ESR1* DNA. n/a = not available

Patient	Days between tissue biopsy and blood draw	Sequencing FFPE tumor tissue	ddPCR plasma for *ESR1* Y537S	ddPCR plasma for *ESR1* Y537N	ddPCR plasma for *ESR1* D538G
ER-positive					
12	-	n/a	Y537S (0.47%)	wild type	wild type
13	0	wild type	wild type	wild type	D538G (0.01%)
14	0	n/a	Y537S (5.02%)	wild type	D538G (2.62%)
15	0	wild type	wild type	wild type	wild type
16	0	wild type	wild type	wild type	D538G (0.01%)
17	0	wild type	wild type	wild type	wild type
18	0	wild type	wild type	wild type	D538G (0.01%)
19	-	n/a	wild type	Y537N (0.06%)	wild type
ER-negative					
20	5	wild type	wild type	wild type	wild type
21	3	wild type	wild type	wild type	wild type
22	0	wild type	wild type	wild type	wild type
23	0	wild type	wild type	wild type	wild type

Table 3.4. Additional patient characteristics

Patient	Tissue	PtDNA	Notes	Tumor burden at blood draw	Oophorectomy	Ovarian Suppression
1	Y537S	Y537S and D538G	underwent an omental biopsy 2009 revealing metastatic lobular carcinoma,	peritoneum with omental nodules, bone	No	No
2	Y537S	Y537S		multiple-skin, bone, liver, ascites, asymptomatic subcutaneous nodules right posterior neck and left upper back	No	Yes
3	D538G	D538G		multiple-bone , liver, post-surgical resection of CNS lesion	No	No
4	Y537S	Y537S	diagnosed with Stage IV disease, site of initial biopsy was right femur which was ER+/PR+/HER2-	multiple - Right breast (primary), bone, liver	No	No
5	D538G	D538G		no evidence of disease	Yes	No
6	D538G	D538G	original tumor in 1992, ER+	multiple-skin, lungs, nodes, brain	No	No
7	D538G	D538G		multiple-bone, liver	No	No
8	Y537N	Y537N	Original tumor in 1998	multiple-liver, lung nodes	No	No
9	wt	D538G		multiple-bone, lymph nodes, spine, sternum, brain lesion, liver, lung	Yes	Yes
10	wt	wt		multiple-bone, soft tissue, lymph nodes, skin	No	No
11	wt	wt		multiple-bone,abdominal lymph nodes, possbly pleura	No	Yes
12	NA	Y537S		bone, liver	No	No
13	wt	D538G		bone	No	No
14	NA	Y537S and D538G		multiple-bone, infiltration of the clivis as well as apparent metastatic deposit in the right pterygoid muscle, pleural disease, right facial region , sclerotic lesions in the right greater wing sphenoid, clivis, occipital condyles and C2 vertebrae. Enhancing soft tissue within the right infratemporal fossa, extending into the right inferior orbital fissure and inferolateral aspect of the extraconal right orbit.	No	Unknown
15	wt	wt	at diagnosis, had 12 cm cancer, started neoadjuvant endocrine therapy	multiple-lung, bone with radiation of T3-T5 and T8-T11, liver	No	Yes
16	wt	D538G	diagnosed with stage IIIB primary peritoneal cancer, difficult to differentiate from metastatic breast cancer, known BRCA2 carrier	multiple-peritioneal, liver	Yes	No
17	wt	wt	metastatic at diagnosis	multiple-bone, liver, pleura	No	Unknown
18	wt	D538G		multiple-lung, liver, ocular metastasis, breast, presternal nodule	No	No
19	NA	Y537N	metastatic at diagnosis, had in breast pCR after 1 year on letrozole, no tissue available	bone only disease-stable after years of endocrine therapy	No	No
20	wt	wt	left inflammatory carcinoma (ER-, PR - HER2+)	multiple-chest wall recurrence, skin nodules, lung, and possibly pleural	No	No
21	wt	wt	inflammatory breast cancer (ER-, PR-, and HER2+)	multiple-pleura, liver, lung, pericardial effusion with tamponade no current issue resolved	No	No
22	wt	wt	metastatic at diagnosis, suggestive of new inflammatory breast cancer	multiple-bone, lung, right pleura, controlateral chest wall soft tissue	No	No
23	wt	wt		multiple-axillary lyph nodes, liver	No	Unknown
wt = wild type						

Table 3.5. Primers used in this study

Pre-amplification Primers	Sequence
Forward	TCCCAGCTCCCATCCTAAAGTG
Reverse	CACTGCGGGCTCTACTTCAT

ddPCR Primers	Sequence
Forward	GCATGAAGTGCAAGAACGTG
Reverse	AGACGGACCAAAGCCACTT

ddPCR Probes	Sequence
ESR1 Y537S	TCTcTGACCTGCTGCTGGAGATGCT
ESR1 Y537N	TCaATGACCTGCTGCTGGAGATGCT
ESR1 D538G	TCTATGgCCTGCTGCTGGAGATGCT
ESR1 WT	TCTATGACCTGCTGCTGGAGATGCT

Cloning Primers	Sequence
Forward	TCCCAGCTCCCATCCTAAAGTG
Reverse	AAAGGATGCATTGCCATAGG

Mutagenesis primers	Sequence
ESR1 Y537S Forward	CCTCTcTGACCTGCTGCTGGA
ESR1 Y537S Reverse	TCCAGCAGCAGGTCAgAGAGG
ESR1 Y537N Forward	CTCaATGACCTGCTGCTGGA
ESR1 Y537N Reverse	TCCAGCAGCAGGTCATtGAG
ESR1 D538G Forward	CCTCTATGgCCTGCTGCTGGA
ESR1 D538G Reverse	TCCAGCAGCAGGcCATAGAGG
ESR1 Y537S D538G Forward	TCTcTGgCCTGCTGCTGGAGAT
ESR1 Y537S D538G Reverse	ATCTCCAGCAGCAGGcCAgAGA

4 Materials and Methods

Isogenic modeling of *ESR1* activating mutations

Cell Culture

The MCF7 cell line[91] and its derivatives were maintained in DMEM media with 5% fetal bovine serum (Life Technologies, Carslbad, CA) and 1% Penicillin-Streptomycin (Life Technologies). For assays involving MCF7 and its derivatives, DMEM:F12 (1:1) media without phenol red was supplemented with 0.5% (serum starved) or 10% (serum supplemented) charcoal dextran stripped fetal bovine serum unless otherwise noted. MCF7 parental and HEK-293T cell lines were purchased from ATCC (Manassas, VA). Parental cell lines were authenticated via short tandem repeat profiling analysis at the Johns Hopkins Genetic Resources Core Facility.

Gene Targeting and Generation of ESR1 Mutation Cell lines

Gene targeting of *ESR1* in MCF7 cells was carried out using recombinant AAV vectors as previously described[70]. Briefly, gene targeting of *ESR1* was carried out using one AAV vector for both the *ESR1* Y537S and D538G mutations. AAV vectors were produced by ligating wild type homology arms generated by PCR into an AAV plasmid backbone (Agilent, La Jolla, CA). Site directed mutagenesis by overlap extension PCR was utilized to generate the *ESR1* Y537S and D538G mutations within the targeting construct. Infectious virus was prepared by co-transfecting HEK-293T cells with pHelper, pRC (Agilent) and the respective *ESR1* mutation carrying rAAV targeting plasmid. Approximately 10^6 cells were used for each viral infection. Targeted neomycin resistant clones were isolated via a modified PCR screening strategy[50] and the cells were then exposed to Cre-expressing recombinant adenovirus to remove the neomycin cassette. All isolated clones were confirmed by Sanger sequencing and droplet digital PCR of genomic DNA and cDNA to ensure the clones harbored the intended *ESR1* mutation as single copies and had equal allelic expression. Single-stranded cDNA was generated using First Strand cDNA Synthesis Kit (Amersham Biosciences). Two clones were isolated for each *ESR1* mutation as well as a targeted wild type control for the *ESR1* exon 10 locus. Primer sequences for PCR amplification, mutagenesis, targeting and sequencing are shown in the Table 2.2-2.8.

Cell proliferation assays

Exponentially growing cells were washed twice with clear HBSS and seeded at a density of $1x10^4$ cells/well in 12 well plates in serum starved media for 24hrs. On day 0, medium was changed to serum supplemented media with and without 1nM β-estradiol (Sigma-Aldrich, St Louis, MO). Medium was changed on day three. Cells were harvested on the indicated dates and counted using a Beckman Coulter counter and the relative proliferation was calculated using the average proliferation for each cell line and the first time point as a reference. Results from the *ESR1* mutant cell lines represent data from two clones unless otherwise noted. All cell lines were counted in triplicate.

Xenograft assays

For each group, five randomly distributed 8- to 10-week-old female athymic nude mice (Harlan Laboratories, Indianapolis, IN), with and without estrogen pellet supplementation, were injected subcutaneously in either flank with $2x10^6$ cells in a 200uL mixture of 80% growth factor reduced Matrigel (BD Biosciences, San Jose, CA) and 20% 1X clear HBSS. For co-inoculations, $1x10^6$ MCF7 cells were combined with either of the $1x10^6$ MCF7 *ESR1* mutant cells before injections. For co-inoculations involving the MCF7 *ESR1* mutants, $1x10^6$ of the MCF7 *ESR1* Y537S mutant cells was combined with $1x10^6$ of the MCF7 *ESR1* D538G mutant cells before injections. Tumor volumes were analyzed at the indicated dates and calculating by multiplying the length, width and height for each tumor volume.

All animal experiments were performed in accordance with institutional and The National Institute of Health Guide for the Care and Use of Laboratory Animal guidelines.

Drug inhibitor assays

Fulvestrant and paclitaxel were obtained from Sigma-Aldrich and were dissolved in dimethyl sulfoxide (DMSO). 4-hydroxytamoxifen was also obtained from Sigma-Aldrich and dissolved in ethanol. Palbociclib was obtained from Selleck (Houston) and dissolved in DMSO. $3x10^3$ cells/well were seeded into 12 well plates and serum starved media for 24hrs. On day 0, media was changed to serum supplemented media with 1nM β-estradiol and the indicated concentration of drug or appropriate vehicle control. Cells were harvested on day 7 and counted using a Beckman Coulter counter. Percent viability was calculated using the average number of cells for each cell line at the indicated concentration normalized to the appropriate vehicle control. Results from the *ESR1* mutant cell lines represent data from two clones unless otherwise noted. All cell lines were counted in triplicate.

Co-culture and co-inoculation assays

For co-culture assays, $1\text{-}2x10^5$ exponentially growing MCF7 cells were seeded with $1\text{-}2x10^5$ exponentially growing MCF7 *ESR1* mutant cells into T25 flask in serum supplemented media with and without 1nM β-estradiol. The same amount of cells was also used for MCF7 *ESR1* Y537S and MCF7 *ESR1* D538G

co-culture experiments. Cells were passaged once a week with 1-2x10^5 cells harvested for genomic DNA extraction at the time points indicated. Genomic DNA was digested and purified for ddPCR analysis.

For co-inoculation studies, animals were euthanized when tumor volumes reached 200-300 cm^3 and xenografts were excised and flash frozen. Tumor xenografts were homogenized with Biomasher tissue grinder (Kimble, Nashville, TN) and resuspended in PBS. Genomic DNA was extracted using QIAamp DNA Blood Mini Kit (Qiagen) and subsequently digested and purified for ddPCR analysis.

Droplet digital PCR

For all droplet digital PCR assays, genomic DNA was digested with CviQ1 restriction enzyme and PCR purified using QIAquick PCR Purification kit (Qiagen) before samples were subjected to ddPCR analysis unless otherwise noted. The QX200 platform (Bio-Rad) was then used for ddPCR per the manufacturer's protocols with the ddPCR primers and probes listed in Table 2.9-2.10. The mutant frequency was determined by the number of mutant DNA alleles to the total (mutant plus wild-type) DNA alleles and the wild type frequency was determined by the number of wild type DNA alleles to total for each sample assayed.

For the co-culture and co-inoculation assays with MCF7 parentals, the mutant and wild type frequency were used to calculate the percentage of MCF7 *ESR1* Y537S and D538G mutant cell lines to MCF7 parental present in each

mixture. For co-inoculations involving the MCF7 *ESR1* mutants, the mutant frequency of *ESR1* Y537S and *ESR1* D583G were used to calculate the percentage of *ESR1* mutants present in each mixture.

Transwells

Exponentially growing cells were washed twice with clear HBSS and seeded at $2x10^3$ cells in 6 well plates or transwell inserts (VWR) in serum supplemented media on day 0. On day 1, cells on the transwells inserts were transferred to the 6 well plates and grown for 13 days. Cells were not passaged and medium was added after one week. Cells were harvested after 13 days and counted using a Beckman Coulter counter. All cell lines were counted in triplicate.

Statistics

All statistical analyses were performed using GraphPad Prism 5 software (GraphPad Software). *Unpaired Student's T tests, 1-way ANOVA and 2-way ANOVA tests were used to compare the experimental groups to the corresponding controls. Significance levels are indicated by the use of one or more asterisk: $P < 0.05$ (*), $P < 0.01$ (**) and $P < 0.001$ (***). Error bars represent +/- SEM.

Detection of *ESR1* mutations in circulating plasma tumor DNA from metastatic breast cancer patients

Patient and sample collection

We conducted this clinical study at the University of Michigan Comprehensive Cancer Center (UMCCC) and the Johns Hopkins Sidney Kimmel Comprehensive Cancer Center (JHSKCCC). Men and women with metastatic (stage IV) breast cancer were eligible. All patients signed informed consent. For the UMCCC cohort, patients were recruited from breast cancer patients undergoing a research tumor biopsy of metastatic disease for whole exome sequencing through UMCCC's MiONCOSEQ program[8, 89]. In particular, these patients were recruited in a companion trial to MiONCOSEQ, designated MiCTC-ONCOSEQ approved by the University of Michigan Health System IRB. Under this protocol, any metastatic breast cancer patients previously enrolled or enrolling in the parent MiONCOSEQ protocol were asked to provide blood samples for ptDNA collected in BCT DNA tubes (Streck) and CTC analyses (data not reported in this publication). For the JHSKCCC cohort, patients were consented and enrolled in an ongoing longitudinal tissue and blood repository protocol, allowing for research use of human tissues and bodily fluids from patients with breast disease. An IRB subprotocol approved for genomic analyses of tumor tissues and blood from breast cancer patients of any stage was used to obtain metastatic tumor biopsies and subsequent blood samples from ER-positive metastatic patients. Metastatic tumor samples obtained as FFPE blocks and slides were sent for NGS DNA analysis using a commercial source (Foundation Medicine). In this cohort, blood samples of 30ml were collected in

EDTA tubes or BCT DNA tubes after patients with *ESR1* mutations were identified. Prospective enrollment is also allowed for this protocol.

Isolation and Quantification of ptDNA for ddPCR

Blood samples and plasma DNA preparation were performed as previously described[82]. Briefly, plasma was obtained by a double spin centrifuge protocol of whole blood to remove cellular contaminants. Blood was centrifuged within 1 hour if collected in EDTA tubes and within 7 days if collected in DNA BCT (Streck) tubes. Purified plasma DNA was isolated using the Qiagen Circulating Nucleic Acid kit (Qiagen) per the manufacturer's protocol. The isolated plasma DNA was then subjected to high fidelity PCR amplification for 10 cycles (Phusion, NEB), using the primers listed in Table 3.6. The PCR amplified products were then diluted and combined with mutant and wild type probes for *ESR1* mutation detection in separate reactions for each mutation specific probe (Table 3.6). The Bio-Rad QX200 platform was then used for ddPCR per the manufacturer's protocol, with results reported as a percentage or fractional abundance of mutant DNA alleles to total (mutant plus wild type) DNA alleles. Samples were run in multiple replicates (at least 8) and results averaged as a meta-well using the QuantaSoft program as previously described[82]. Positive and negative controls were included for each assay to control for proper signal gating and exclusion of contamination artifacts. At least 10,000 genome equivalents were assayed for each patient sample, and negative samples were scored as negative only after assaying 100,000 genome equivalents.

Synthetic Template Synthesis

To construct the Y537S, Y537N, D538G and Y537S + D538G synthetic templates for specificity controls, a ~1kb genomic DNA fragment of the ESR1 LBD was amplified by PCR and ligated into the pSEPT vector[92]. PCR site directed mutagenesis[93] was then carried out for each mutation with primers designed for overlapping PCR extension to generate all single mutation synthesis templates (pY537S, pY537N, pD538G). Once generated, the pY537S template was utilized to create the pY537S+D538G using dual mutation primers. All templates were confirmed by Sanger sequencing. Primer sequences for PCR are provided in Table 3.6.

Statistical Analysis

In order to quantify the percent ptDNA containing mutant *ESR1* in plasma samples, a fractional abundance calculation using the QuantaSoft program (Bio-Rad Technologies) was employed, using the total number of droplets (with and without DNA) to calculate the number of DNA molecules as copies/µl, and then dividing the number of mutant DNA molecules by the number of total DNA molecules (mutant plus wild type), multiplied by 100 to yield a percentage of mutant DNA molecules in a sample taking into account a Poisson distribution of occupied to unoccupied droplets. For cohort 2, Fisher's exact two-tailed test (GraphPad) was used to calculate differences in *ESR1* mutation status (mutant vs. wild type) between tissue and blood using a 2x2 contingency table with 9 samples for tissue and 12 samples for blood.

References

1. Siegel RL, Miller KD, Jemal A. Cancer statistics, 2017. CA: A Cancer Journal for Clinicians 2017;67:7-30.

2. Group USCSW. United States Cancer Statistics: 1999–2013 Incidence and Mortality Web-based Report. US Department of Health and Human Services, Centers for Disease Control and Prevention and National Cancer Institute 2016.

3. Vogelstein B, Kinzler KW. Cancer genes and the pathways they control. Nat Med 2004;10:789-99.

4. Tavassoli FA DP. World Health Organization Classification of Tumors: Pathology and Genetics of Tumors of the Breast and Female Genital Organs IARC Press 2003.

5. Alteri R CB. Breast Cancer Facts & Figures 2015-2016. American Cancer Society 2016.

6. Li S, Shen D, Shao J, et al. Endocrine-therapy-resistant ESR1 variants revealed by genomic characterization of breast-cancer-derived xenografts. Cell Rep 2013;4:1116-30.

7. Toy W, Shen Y, Won H, et al. ESR1 ligand-binding domain mutations in hormone-resistant breast cancer. Nat Genet 2013;45:1439-45.

8. Robinson DR, Wu YM, Vats P, et al. Activating ESR1 mutations in hormone-resistant metastatic breast cancer. Nat Genet 2013;45:1446-51.

9. Jeselsohn R, Yelensky R, Buchwalter G, et al. Emergence of constitutively active estrogen receptor-alpha mutations in pretreated advanced estrogen receptor-positive breast cancer. Clin Cancer Res 2014;20:1757-67.

10. Merenbakh-Lamin K, Ben-Baruch N, Yeheskel A, et al. D538G mutation in estrogen receptor-alpha: A novel mechanism for acquired endocrine resistance in breast cancer. Cancer Res 2013;73:6856-64.

11. Beatson GT. On the treatment of inoperable cases of carcinoma of the mamma: suggestions for a new method of treatment with illustrative cases. Lancet 1896;2:104-407.

12. Boyd S. On oophorectomy in cancer of the breast. BMJ 1900;2:1161-7.

13. Allen E, Doisy EA. An ovarian hormone. Preliminary report on its localization, extraction and partial purification, and action in test animals. . JAMA 1923;250:2681-3.

14. EV Jensen HJ. Fate of steroid estrogens in target tissues. Biological Activities of Steroids in Relation to Cancer 1960:161-74.

15. Greene GL, Nolan C, Engler JP, Jensen EV. Monoclonal antibodies to human estrogen receptor. Proc Natl Acad Sci U S A 1980;77:5115-9.

16. Walter P, Green S, Greene G, et al. Cloning of the human estrogen receptor cDNA. Proc Natl Acad Sci U S A 1985;82:7889-93.

17. Green S, Walter P, Kumar V, et al. Human oestrogen receptor cDNA: sequence, expression and homology to v-erb-A. Nature 1986;320:134-9.

18. Mosselman S, Polman J, Dijkema R. ER beta: identification and characterization of a novel human estrogen receptor. FEBS Lett 1996;392:49-53.

19. Krust A, Green S, Argos P, et al. The chicken oestrogen receptor sequence: homology with v-erbA and the human oestrogen and glucocorticoid receptors. EMBO J 1986;5:891-7.

20. Green S, Kumar V, Krust A, Walter P, Chambon P. Structural and functional domains of the estrogen receptor. Cold Spring Harb Symp Quant Biol 1986;51 Pt 2:751-8.

21. Tora L, White J, Brou C, et al. The human estrogen receptor has two independent nonacidic transcriptional activation functions. Cell 1989;59:477-87.

22. Metivier R, Penot G, Flouriot G, Pakdel F. Synergism between ERalpha transactivation function 1 (AF-1) and AF-2 mediated by steroid receptor coactivator protein-1: requirement for the AF-1 alpha-helical core and for a direct interaction between the N- and C-terminal domains. Mol Endocrinol 2001;15:1953-70.

23. Montano MM, Muller V, Trobaugh A, Katzenellenbogen BS. The carboxy-terminal F domain of the human estrogen receptor: role in the transcriptional activity of the receptor and the effectiveness of antiestrogens as estrogen antagonists. Mol Endocrinol 1995;9:814-25.

24. Yang J, Singleton DW, Shaughnessy EA, Khan SA. The F-domain of estrogen receptor-alpha inhibits ligand induced receptor dimerization. Mol Cell Endocrinol 2008;295:94-100.

25. Bolger R, Wiese TE, Ervin K, Nestich S, Checovich W. Rapid screening of environmental chemicals for estrogen receptor binding capacity. Environ Health Perspect 1998;106:551-7.

26. O'Lone R, Frith MC, Karlsson EK, Hansen U. Genomic targets of nuclear estrogen receptors. Mol Endocrinol 2004;18:1859-75.

27. Safe S, Kim K. Non-classical genomic estrogen receptor (ER)/specificity protein and ER/activating protein-1 signaling pathways. J Mol Endocrinol 2008;41:263-75.

28. Gottlicher M, Heck S, Herrlich P. Transcriptional cross-talk, the second mode of steroid hormone receptor action. J Mol Med (Berl) 1998;76:480-9.

29. Likhite VS, Stossi F, Kim K, Katzenellenbogen BS, Katzenellenbogen JA. Kinase-specific phosphorylation of the estrogen receptor changes receptor interactions with ligand, deoxyribonucleic acid, and coregulators associated with alterations in estrogen and tamoxifen activity. Mol Endocrinol 2006;20:3120-32.

30. Anbalagan M, Rowan BG. Estrogen receptor alpha phosphorylation and its functional impact in human breast cancer. Mol Cell Endocrinol 2015;418 Pt 3:264-72.

31. Losel R, Wehling M. Nongenomic actions of steroid hormones. Nat Rev Mol Cell Biol 2003;4:46-56.

32. Migliaccio A, Di Domenico M, Castoria G, et al. Tyrosine kinase/p21ras/MAP-kinase pathway activation by estradiol-receptor complex in MCF-7 cells. EMBO J 1996;15:1292-300.

33. Castoria G, Migliaccio A, Bilancio A, et al. PI3-kinase in concert with Src promotes the S-phase entry of oestradiol-stimulated MCF-7 cells. EMBO J 2001;20:6050-9.

34. Sorlie T, Tibshirani R, Parker J, et al. Repeated observation of breast tumor subtypes in independent gene expression data sets. Proc Natl Acad Sci U S A 2003;100:8418-23.

35. Carey LA, Perou CM, Livasy CA, et al. Race, breast cancer subtypes, and survival in the Carolina Breast Cancer Study. JAMA 2006;295:2492-502.

36. Frasor J, Stossi F, Danes JM, Komm B, Lyttle CR, Katzenellenbogen BS. Selective estrogen receptor modulators: discrimination of agonistic versus antagonistic activities by gene expression profiling in breast cancer cells. Cancer Res 2004;64:1522-33.

37. Jordan VC. The science of selective estrogen receptor modulators: concept to clinical practice. Clin Cancer Res 2006;12:5010-3.

38. Dowsett M, Nicholson RI, Pietras RJ. Biological characteristics of the pure antiestrogen fulvestrant: overcoming endocrine resistance. Breast Cancer Res Treat 2005;93 Suppl 1:S11-8.

39. Lonning PE, Eikesdal HP. Aromatase inhibition 2013: clinical state of the art and questions that remain to be solved. Endocr Relat Cancer 2013;20:R183-201.

40. Encarnacion CA, Ciocca DR, McGuire WL, Clark GM, Fuqua SA, Osborne CK. Measurement of steroid hormone receptors in breast cancer patients on tamoxifen. Breast Cancer Res Treat 1993;26:237-46.

41. Gutierrez MC, Detre S, Johnston S, et al. Molecular changes in tamoxifen-resistant breast cancer: relationship between estrogen receptor, HER-2, and p38 mitogen-activated protein kinase. J Clin Oncol 2005;23:2469-76.

42. Lipton A, Leitzel K, Ali SM, et al. Serum HER-2/neu conversion to positive at the time of disease progression in patients with breast carcinoma on hormone therapy. Cancer 2005;104:257-63.

43. Meng S, Tripathy D, Shete S, et al. HER-2 gene amplification can be acquired as breast cancer progresses. Proc Natl Acad Sci U S A 2004;101:9393-8.

44. Arpino G, Weiss H, Lee AV, et al. Estrogen receptor-positive, progesterone receptor-negative breast cancer: association with growth factor receptor expression and tamoxifen resistance. J Natl Cancer Inst 2005;97:1254-61.

45. Brankovic-Magic M, Jankovic R, Neskovic-Konstantinovic Z, Nikolic-Vukosavljevic D. Progesterone receptor status of breast cancer metastases. J Cancer Res Clin Oncol 2002;128:55-60.

46. Wood LD, Parsons DW, Jones S, et al. The genomic landscapes of human breast and colorectal cancers. Science 2007;318:1108-13.

47. Sjoblom T, Jones S, Wood LD, et al. The consensus coding sequences of human breast and colorectal cancers. Science 2006;314:268-74.

48. Comprehensive molecular portraits of human breast tumours. Nature 2012;490:61-70.

49. Zhang QX, Borg A, Wolf DM, Oesterreich S, Fuqua SA. An estrogen receptor mutant with strong hormone-independent activity from a metastatic breast cancer. Cancer Res 1997;57:1244-9.

50. Konishi H, Karakas B, Abukhdeir AM, et al. Knock-in of mutant K-ras in nontumorigenic human epithelial cells as a new model for studying K-ras mediated transformation. Cancer Res 2007;67:8460-7.

51. Bose R, Kavuri SM, Searleman AC, et al. Activating HER2 mutations in HER2 gene amplification negative breast cancer. Cancer Discov 2013;3:224-37.

52. Zabransky DJ, Yankaskas CL, Cochran RL, et al. HER2 missense mutations have distinct effects on oncogenic signaling and migration. Proc Natl Acad Sci U S A 2015;112:E6205-14.

53. Di Nicolantonio F, Arena S, Gallicchio M, et al. Replacement of normal with mutant alleles in the genome of normal human cells unveils mutation-specific drug responses. Proc Natl Acad Sci U S A 2008;105:20864-9.

54. Lauring J, Cosgrove DP, Fontana S, et al. Knock in of the AKT1 E17K mutation in human breast epithelial cells does not recapitulate oncogenic PIK3CA mutations. Oncogene 2010;29:2337-45.

55. Wang GM, Wong HY, Konishi H, et al. Single copies of mutant KRAS and mutant PIK3CA cooperate in immortalized human epithelial cells to induce tumor formation. Cancer Res 2013;73:3248-61.

56. Di Nicolantonio F, Arena S, Tabernero J, et al. Deregulation of the PI3K and KRAS signaling pathways in human cancer cells determines their response to everolimus. J Clin Invest 2010;120:2858-66.

57. Finn RS, Dering J, Conklin D, et al. PD 0332991, a selective cyclin D kinase 4/6 inhibitor, preferentially inhibits proliferation of luminal estrogen receptor-positive human breast cancer cell lines in vitro. Breast Cancer Res 2009;11:R77.

58. (EBCTCG) EBCTCG. Effects of chemotherapy and hormonal therapy for early breast cancer on recurrence and 15-year survival: an overview of the randomised trials. Lancet 2005;365:1687-717.

59. Riggins RB, Schrecengost RS, Guerrero MS, Bouton AH. Pathways to tamoxifen resistance. Cancer Lett 2007;256:1-24.

60. Lauring J, Park BH, Wolff AC. The phosphoinositide-3-kinase-Akt-mTOR pathway as a therapeutic target in breast cancer. J Natl Compr Canc Netw 2013;11:670-8.

61. Brooks SC, Locke ER, Soule HD. Estrogen receptor in a human cell line (MCF-7) from breast carcinoma. J Biol Chem 1973;248:6251-3.

62. Cristofanilli M, Turner NC, Bondarenko I, et al. Fulvestrant plus palbociclib versus fulvestrant plus placebo for treatment of hormone-receptor-positive, HER2-negative metastatic breast cancer that progressed on previous endocrine therapy (PALOMA-3): final analysis of the multicentre, double-blind, phase 3 randomised controlled trial. Lancet Oncol 2016;17:425-39.

63. Hua VY, Wang WK, Duesberg PH. Dominant transformation by mutated human ras genes in vitro requires more than 100 times higher expression than is observed in cancers. Proc Natl Acad Sci U S A 1997;94:9614-9.

64. Finn RS, Crown JP, Lang I, et al. The cyclin-dependent kinase 4/6 inhibitor palbociclib in combination with letrozole versus letrozole alone as first-line treatment of oestrogen receptor-positive, HER2-negative, advanced breast cancer (PALOMA-1/TRIO-18): a randomised phase 2 study. Lancet Oncol 2015;16:25-35.

65. Wardell SE, Ellis MJ, Alley HM, et al. Efficacy of SERD/SERM Hybrid-CDK4/6 Inhibitor Combinations in Models of Endocrine Therapy-Resistant Breast Cancer. Clin Cancer Res 2015;21:5121-30.

66. Zhao L, Vogt PK. Helical domain and kinase domain mutations in p110alpha of phosphatidylinositol 3-kinase induce gain of function by different mechanisms. Proc Natl Acad Sci U S A 2008;105:2652-7.

67. Yasuda H, Park E, Yun CH, et al. Structural, biochemical, and clinical characterization of epidermal growth factor receptor (EGFR) exon 20 insertion mutations in lung cancer. Sci Transl Med 2013;5:216ra177.

68. Fanning SW, Mayne CG, Dharmarajan V, et al. Estrogen receptor alpha somatic mutations Y537S and D538G confer breast cancer endocrine resistance by stabilizing the activating function-2 binding conformation. Elife 2016;5.

69. Beaver JA, Gustin JP, Yi KH, et al. PIK3CA and AKT1 mutations have distinct effects on sensitivity to targeted pathway inhibitors in an isogenic luminal breast cancer model system. Clin Cancer Res 2013;19:5413-22.

70. Gustin JP, Karakas B, Weiss MB, et al. Knockin of mutant PIK3CA activates multiple oncogenic pathways. Proc Natl Acad Sci U S A 2009;106:2835-40.

71. Croessmann S, Wong HY, Zabransky DJ, et al. PIK3CA mutations and TP53 alterations cooperate to increase cancerous phenotypes and tumor heterogeneity. Breast Cancer Res Treat 2017.

72. Gerlinger M, Rowan AJ, Horswell S, et al. Intratumor heterogeneity and branched evolution revealed by multiregion sequencing. N Engl J Med 2012;366:883-92.

73. Rothe F, Laes JF, Lambrechts D, et al. Plasma circulating tumor DNA as an alternative to metastatic biopsies for mutational analysis in breast cancer. Ann Oncol 2014;25:1959-65.

74. Lebofsky R, Decraene C, Bernard V, et al. Circulating tumor DNA as a non-invasive substitute to metastasis biopsy for tumor genotyping and personalized medicine in a prospective trial across all tumor types. Mol Oncol 2015;9:783-90.

75. Jeselsohn R, Yelensky R, Buchwalter G, et al. Emergence of constitutively active estrogen receptor-alpha mutations in pretreated advanced estrogen receptor positive breast cancer. Clin Cancer Res 2014.

76. Leary RJ, Kinde I, Diehl F, et al. Development of personalized tumor biomarkers using massively parallel sequencing. Sci Transl Med 2010;2:20ra14.

77. Higgins MJ, Jelovac D, Barnathan E, et al. Detection of tumor PIK3CA status in metastatic breast cancer using peripheral blood. Clin Cancer Res 2012;18:3462-9.

78. Leary RJ, Sausen M, Kinde I, et al. Detection of chromosomal alterations in the circulation of cancer patients with whole-genome sequencing. Sci Transl Med 2012;4:162ra54.

79. Forshew T, Murtaza M, Parkinson C, et al. Noninvasive identification and monitoring of cancer mutations by targeted deep sequencing of plasma DNA. Sci Transl Med 2012;4:136ra68.

80. Chan KC, Jiang P, Chan CW, et al. Noninvasive detection of cancer-associated genome-wide hypomethylation and copy number aberrations by plasma DNA bisulfite sequencing. Proc Natl Acad Sci U S A 2013;110:18761-8.

81. Murtaza M, Dawson SJ, Tsui DW, et al. Non-invasive analysis of acquired resistance to cancer therapy by sequencing of plasma DNA. Nature 2013;497:108-12.

82. Beaver JA, Jelovac D, Balukrishna S, et al. Detection of cancer DNA in plasma of patients with early-stage breast cancer. Clin Cancer Res 2014;20:2643-50.

83. Bettegowda C, Sausen M, Leary RJ, et al. Detection of circulating tumor DNA in early- and late-stage human malignancies. Sci Transl Med 2014;6:224ra24.

84. Stroun M, Maurice P, Vasioukhin V, et al. The origin and mechanism of circulating DNA. Ann N Y Acad Sci 2000;906:161-8.

85. Choi JJ, Reich CF, 3rd, Pisetsky DS. The role of macrophages in the in vitro generation of extracellular DNA from apoptotic and necrotic cells. Immunology 2005;115:55-62.

86. Diehl F, Schmidt K, Choti MA, et al. Circulating mutant DNA to assess tumor dynamics. Nat Med 2008;14:985-90.

87. Diaz LA, Jr., Williams RT, Wu J, et al. The molecular evolution of acquired resistance to targeted EGFR blockade in colorectal cancers. Nature 2012;486:537-40.

88. Misale S, Yaeger R, Hobor S, et al. Emergence of KRAS mutations and acquired resistance to anti-EGFR therapy in colorectal cancer. Nature 2012;486:532-6.

89. Roychowdhury S, Iyer MK, Robinson DR, et al. Personalized oncology through integrative high-throughput sequencing: a pilot study. Sci Transl Med 2011;3:111ra21.

90. Oesterreich S, Davidson NE. The search for ESR1 mutations in breast cancer. Nat Genet 2013;45:1415-6.

91. Brooks AL, Mead DK, Peters RF. Effect of aging on the frequency of metaphase chromosome aberrations in the liver of the Chinese hamster. J Gerontol 1973;28:452-4.

92. Topaloglu O, Hurley PJ, Yildirim O, Civin CI, Bunz F. Improved methods for the generation of human gene knockout and knockin cell lines. Nucleic Acids Res 2005;33:e158.

93. Ho SN, Hunt HD, Horton RM, Pullen JK, Pease LR. Site-directed mutagenesis by overlap extension using the polymerase chain reaction. Gene 1989;77:51-9.

Curriculum Vitae

David Chu
1650 Orleans Street, CRB1 Rm. 116, Baltimore MD 21287

818.357.8855 | dchu21@jhmi.edu

EDUCATION

Johns Hopkins University, School of Medicine, Baltimore, MD 2011-2017
Ph.D. in Cellular and Molecular Medicine

Thesis Dissertation: *ESR1* mutations and Modeling Endocrine Resistance in Estrogen Receptor Positive Breast Cancer

Thesis Advisor: Ben Ho Park, MD., Ph.D.

University of California, Los Angeles, Los Angeles, CA 2004-2008

B.S Biochemistry

cum laude

RESEARCH EXPERIENCE

Johns Hopkins University, School of Medicine 2011-2016
Ph.D. Graduate Student, Park Laboratory
Baltimore, MD

Developed and designed a liquid biopsy assay using droplet digital PCR (ddPCR) to detect rare somatic alterations associated with hormone therapy resistance in the plasma of patients with metastatic, ER-positive breast cancer. Additionally, created and functionally characterized cell line models for mutations associated with hormone therapy resistance in ER-positive breast cancer. Lastly, mentored and trained undergraduate, graduate and medical fellow trainees.

Cedars-Sinai Medical Center 2009-2011
Research Associate I, Medina-Kauwe Laboratory Los Angeles, CA

Assisted in the completion of a project investigating the stability, targeting and mechanistic properties of the HerPBK10-doxorubcin conjugate (Her-Dox) in a HER2+ cell line model. Contributed to an ongoing project concerning the therapeutic efficacy and safety of using a HerPBK10- gallium(II) corrole conjugate (HerGa) to target HER2+

cell lines both *in vitro* and *in vivo*. Investigated the targeting and silencing properties of a HerPBK10-Her2 siRNA conjugate to HER2+ cells *in vitro* and *in vivo* to downregulate HER2 and assess cell viability and tumor regression.

University of California, Los Angeles 2005-2008
Undergraduate Researcher, Lee Lab Los Angeles, CA

Assisted with the discovery of the single amino acid responsible for the difference in binding affinities between Nipah and Hendra attachment protein (NiV-G/HeV-G) to the cellular receptors, ephrinB2 and ephrinB3. Pioneered a project aimed to elucidate the step during Nipah viral entry where NiV-G cysteine mutants manifest their fusion deficient phenotype in ephrinB2 expressing 293T and CHO cell lines.

AWARDS AND HONORS

Vice Provost's Recognition Award for Undergraduate research	2007, 2008
Undergraduate Research Scholars Program	2007 – 2008
Undergraduate Research Fellows Program	2006 - 2007
Dean's Honor List	Winter 2006, 2008; Spring 2006 – 2008
Change A Life Foundation Recipient	2005-2008

MENTORSHIP

Trained the following individuals during their time in the lab

Bracha Erlanger – current member of the Park lab at Johns Hopkins SOM

Karen Cravero – current member of the Park lab at Johns Hopkins SOM

Patricia Valda Toro – medical student, Yale School of Medicine

Justin Lee – MSTP student, UCLA School of Medicine

Ian Waters – current member of the Park lab at Johns Hopkins SOM

Alessandro Leal – graduate student in Velculescu lab at Johns Hopkins SOM

Fatima Boftas – undergraduate student at Johns Hopkins University

PUBLICATIONS

Croessmann S, Wong HY, Zabransky DJ**, Chu D**, Rosen DM, Cidado J, Cochran RL, Dalton WB, Erlanger B, Cravero K, Button B, Kyker-Snowman K, Hurley PJ, Lauring J, Park BH. PIK3CA mutations and TP53 alterations cooperate to increase cancerous phenotypes and tumor heterogeneity. Breast Cancer Res Treat. 2017 Feb 11

Goldstein A, Valda Toro P, Lee J, Silberstein JL, Nakazawa M, Waters I, Cravero K, **Chu D**, Cochran RL, Kim M, Shinn D, Torquato S, Hughes RM, Pallavajjala A, Carducci MA, Paller CJ, Denmeade SR, Kressel B, Trock BJ, Eisenberger MA, Antonarakis ES, Park BH, Hurley PJ. Detection fidelity of AR mutations in plasma derived cell-free DNA. Oncotarget. 2017 Jan 31

Lee J, Axilbund J, Dalton WB, Laheru D, Watkins S, **Chu D**, Cravero K, Button B, Kyker-Snowman K, Waters I, Gocke CD, Lauring J, Park BH A Polycythemia Vera JAK2 Mutation Masquerading as a Duodenal Cancer Mutation. J Natl Compr Canc Netw. 2016 Dec 14(12):1495-1498

*Scott GK, ***Chu D**, Kaur R, Malato J, Rothschild DE, Frazier K, Eppenberger-Castori S, Hann B, Park BH, Benz CC. ERpS294 is a biomarker of ligand or mutational ERα activation and a breast cancer target for CDK2 inhibition. Oncotarget. 2016 Oct 18

(*these authors contributed equally to this work)

Parsons HA, Beaver JA, Cimino-Mathews A, Ali SM, Axilbund J, **Chu D**, Connolly R, Cochran R, Croessmann S, Clark T, Gocke CD, Jeter SC, Kennedy M, Lauring J, Lee J, Lipson D, Miller V, Otto G, Rosner GL, Ross JS, Slater SA, Stephens PJ, VanDenBerg DA, Wolff AC, Young L, Zabansky DJ, Zhang Z, Zorzi J, Stearns V, Park BH. Individualized Molecular Analyses Guide Efforts (IMAGE): A Prospective Study of Molecular Profiling of Tissue and Blood in Metastatic Triple Negative Breast Cancer. Clin Cancer Res. 2016 Aug 3

Hayashi M, **Chu D**, Meyer CF, Llosa NJ, McCarty G, Morris CD, Levin AS, Wolinsky JP, Albert CM, Steppan DA, Park BH, Loeb DM. Highly personalized detection of minimal Ewing sarcoma disease burden from plasma tumor DNA. Cancer. 2016 Jun 28

Cidado J, Wong HY, Rosen DM, Cimino-Mathews A, Garay JP, Fessler AG, Rasheed ZA, Hicks J, Cochran RL, Croessmann S, Zabransky DJ, Mohseni M, Beaver JA, **Chu D**, Cravero K, Christenson ES, Medford A, Mattox A, De Marzo AM, Argani P, Chawla A, Hurley PJ, Lauring J, Park BH. Ki-67 is required for maintenance of cancer stem cells but not cell proliferation. Oncotarget. 2016 Feb 2;7(5):6281-93

Wong HY, Wang GM, Croessmann S, Zabransky DJ, **Chu D**, Garay JP, Cidado J, Cochran RL, Beaver JA, Aggarwal A, Liu ML, Argani P, Meeker A, Hurley PJ, Lauring J, Park BH. TMSB4Y is a candidate tumor suppressor on the Y chromosome and is deleted in male breast cancer. Oncotarget. 2015 Dec 29;6(42):44927-40

Zabransky DJ, Yankaskas CL, Cochran RL, Wong HY, Croessmann S, **Chu D**, Kavuri SM, Red Brewer M, Rosen DM, Dalton WB, Cimino-Mathews A, Cravero K, Button B, Kyker-Snowman K, Cidado J, Erlanger B, Parsons HA, Manto KM, Bose R, Lauring J, Arteaga CL, Konstantopoulos K, Park BH. HER2 missense mutations have distinct effects on oncogenic signaling and migration. Proc Natl Acad Sci USA. 2015 Nov 10;112(45)

Croessmann S, Wong HY, Zabransky DJ, **Chu D**, Mendonca J, Sharma A, Mohseni M, Rosen DM, Scharpf RB, Cidado J, Cochran RL, Parsons HA, Dalton WB, Erlanger B, Button B, Cravero K, Kyker-Snowman K, Beaver JA, Kachhap S, Hurley PJ, Lauring J, Park BH. NDRG1 links p53 with proliferation-mediated centrosome homeostasis and genome stability. Proc Natl Acad Sci U S A. 2015 Sep 15;112(37)

***Chu D**, *Paoletti C, Gersch C, VanDenBerg DA, Zabransky DJ, Cochran RL, Wong HY, Toro PV, Cidado J, Croessmann S, Erlanger B, Cravero K, Kyker-Snowman K, Button B, Parsons HA, Dalton WB, Gillani R, Medford A, Aung K, Tokudome N, Chinnaiyan AM, Schott A, Robinson D, Jacks KS, Lauring J, Hurley PJ, Hayes DF, Rae JM, Park BH. ESR1 Mutations in Circulating Plasma Tumor DNA from Metastatic Breast Cancer Patients. Clin Cancer Res. 2015 Aug 10

(*these authors contributed equally to this work)

Cochran RL, Cidado J, Kim M, Zabransky DJ, Croessmann S, **Chu D**, Wong HY, Beaver JA, Cravero K, Erlanger B, Parsons H, Heaphy CM, Meeker AK, Lauring J, Park BH. Functional isogenic modeling of BRCA1 alleles reveals distinct carrier phenotypes. Oncotarget. 2015 Sep 22;6(28)

Toro PV, Erlanger B, Beaver JA, Cochran RL, VanDenBerg DA, Yakim E, Cravero K, **Chu D**, Zabransky DJ, Wong HY, Croessmann S, Parsons H, Hurley PJ, Lauring J, Park BH. Comparison of cell stabilizing blood collection tubes for circulating plasma tumor DNA. Clin Biochem. 2015 Oct;48(15):993-8

Blair BG, Wu X, Zahari MS, Mohseni M, Cidado J, Wong HY, Beaver JA, Cochran RL, Zabransky DJ, Croessmann S, **Chu D**, Toro PV, Cravero K, Pandey A, Park BH. A phosphoproteomic screen demonstrates differential dependence on HER3 for MAP kinase pathway activation by distinct PIK3CA mutations. Proteomics. 2015 Jan;15(2-3):318-26

Cochran RL, Cravero K, **Chu D**, Erlanger B, Toro PV, Beaver JA, Zabransky DJ, Wong HY, Cidado J, Croessmann S, Parsons HA, Kim M, Wheelan SJ, Argani P, Park BH. Analysis of BRCA2 loss of heterozygosity in tumor tissue using droplet digital polymerase chain reaction. Hum Pathol. 2014 Jul;45(7):1546-50.

Beaver JA, Jelovac D, Balukrishna S, Cochran RL, Croessmann S, Zabransky DJ, Wong HY, Valda Toro P, Cidado J, Blair BG, **Chu D**, Burns T, Higgins MJ, Stearns V, Jacobs L, Habibi M, Lange J, Hurley PJ, Lauring J, VanDenBerg DA, Kessler J, Jeter S, Samuels ML, Maar D, Cope L, Cimino-Mathews A, Argani P, Wolff AC, Park BH. Detection of cancer DNA in plasma of patients with early-stage breast cancer. Clin Cancer Res. 2014 May 15;20(10):2643-50.

Hwang JY, Lubow DJ, **Chu D**, Sims J, Alonso-Valenteen F, Gray HB, Gross Z, Farkas DL, Medina-Kauwe LK. Photoexcitation of tumor-targeted corroles induces singlet oxygen-mediated augmentation of cytotoxicity. J Control Release. 2012 Nov 10;163(3):368-73

Maar D, Harmon B, **Chu D**, Schulz B, Aguilar H, Lee B. Cysteines in the stalk of the Nipah virus G glycoprotein are located in a distinct subdomain critical for fusion activation. J. Virology 2012, Jun;86(12):6632-42

Hwang JY, Park J, Kang BJ, Lubow DJ, **Chu D**, Farkas DL, Shung KK, Medina-Kauwe LK. Multimodality imaging in vivo for preclinical assessment of tumor-targeted doxorubicin nanoparticles. PLoS One. 2012;7(4):e34463

Agadjanian H, **Chu D**, Hwang JY, Wachsmann-Hogiu S, Rentsendorj A, Song L, Valluripalli V, Lubow J, Ma J, Sharifi B, Farkas DL, Medina-Kauwe LK. Chemotherapy targeting by DNA capture in viral protein particles. Nanomedicine 2012, 2012 Mar;7(3):335-52

Hwang JY, Lubow J, **Chu D**, Ma J, Agadjanian H, Gray HB, Gross Z, Farkas DL, Medina-Kauwe LK. A Mechanistic Study of Tumor-Targeted Corrole Cytotoxicity. Molecular Pharmaceutics 2011. Dec 5;8(6):2233-43

Hwang JY, Lubow J, **Chu D**, Gross Z, Gray HB, Farkas DL, Medina-Kauwe LK. Investigating the photosensitizer-potential of targeted gallium corrole using multimode optical imaging. Proc SPIE Int Soc Opt Eng. 2011 Jan 22

Negrete OA, **Chu D**, Aguilar HC, Lee B. Single amino acid changes in the Nipah and Hendra virus attachment glycoproteins distinguish ephrinB2 from ephrinB3 usage. J. Virology 2007 81(19), 10804-10814

CONFERENCE POSTERS

Cedars-Sinai Medical Center Research Institute Second Annual Research Day (2011)

Targeting siRNA toxicity to HER2+ tumors. **Chu D**, Lubow J, Hwang JY, Rentsendorj A, Beach J, Valluripalli V, Agadjanian H, Ma J, Medina-Kauwe LK.

Cedars-Sinai Medical Center Research Institute Annual Research Day (2010)

Investigating drug mechanism of targeted gallium corrole and its potential as a photosensitizer using multimode optical imaging. Lubow J, Hwang JY, **Chu D**, Gross Z, Gray HB, Farkas DL, Medina-Kauwe LK.

11th Annual Science Poster Day, Los Angeles, CA (2008)
Cysteines in stalk domain of Nipah virus attachment protein G are important for oligomeric stability and fusion promotion. **Chu D,** Negrete OA, Schulz B, Lee B.

10th Annual Science Poster Day, Los Angeles, CA (2007)
Cysteines in the stalk domain of the attachment protein for the Nipah virus are critical for viral entry. **Chu D**, Negrete OA, Lee B.

INVENTION DISCLOSURES

ESR1 Mutations in Human Breast Cancer Cells. Park, B.H., and Chu, D. (Disclosure filed January 2016)